


Summer 8-18-2017

Using Hydroacoustics to Investigate Biological Responses in Fish Abundance to Restoration Efforts in the Penobscot River, Maine

Constantin C. Scherelis

University of Maine, constantin.scherelis@maine.edu

Follow this and additional works at: <https://digitalcommons.library.umaine.edu/etd>

 Part of the [Biostatistics Commons](#), [Environmental Indicators and Impact Assessment Commons](#), [Environmental Monitoring Commons](#), [Fresh Water Studies Commons](#), [Numerical Analysis and Scientific Computing Commons](#), and the [Other Physics Commons](#)

Recommended Citation

Scherelis, Constantin C., "Using Hydroacoustics to Investigate Biological Responses in Fish Abundance to Restoration Efforts in the Penobscot River, Maine" (2017). *Electronic Theses and Dissertations*. 2748.
<https://digitalcommons.library.umaine.edu/etd/2748>

This Open-Access Thesis is brought to you for free and open access by DigitalCommons@UMaine. It has been accepted for inclusion in Electronic Theses and Dissertations by an authorized administrator of DigitalCommons@UMaine. For more information, please contact um.library.technical.services@maine.edu.

**USING HYDROACOUSTICS TO INVESTIGATE BIOLOGICAL RESPONSES
IN FISH ABUNDANCE TO RESTORATION EFFORTS
IN THE PENOBSCOT RIVER, MAINE**

By Constantin C. Scherelis

B.S. University of Tennessee, 2014

A THESIS

Submitted in Partial Fulfillment of the

Requirements for the Degree of

Master of Science

(in Oceanography)

The Graduate School

The University of Maine

August 2017

Advisory Committee:

Dr. Gayle Zydlewski, Associate Professor of Marine Science, Advisor

Dr. Damian Brady, Assistant Professor of Oceanography

Dr. Neal Pettigrew, Professor of Oceanography

**USING HYDROACOUSTICS TO INVESTIGATE BIOLOGICAL RESPONSES
IN FISH ABUNDANCE TO RESTORATION EFFORTS
IN THE PENOBSCOT RIVER, MAINE**

By Constantin C. Scherelis

Thesis Advisor: Dr. Gayle Zydlewski

An Abstract of the Thesis Presented in
Partial Fulfillment of the Requirements for the
Degree of Master of Science
(in Oceanography)
August 2017

Spatiotemporal advantages linked to hydroacoustic sampling techniques have caused a surge in the use of these techniques for fisheries monitoring studies applied over long periods of time in marine systems. Dynamic physical conditions such as tidal height, boat traffic, floating debris, and suspended particle concentrations result in unwanted noise signatures that vary in intensity and location within a hydroacoustic beam over time and can be mixed with the acoustic returns from intended targets (e.g., fish). Typical processing filters applied over long term datasets to minimize noise and maximize signals do not address spatiotemporal fluctuations of noise in dynamic systems. We present a methodological approach to obtain fish counts from large hydroacoustic datasets collected in dynamic systems by 1) developing an automated processing algorithm that imposes spatially and temporally varying noise thresholds according to the signal-to-noise ratio present, 2) creating a fish count index standardized to the noise conditions present at the time of detection, and 3) validating the applied algorithm by manually quantifying the margins of error of automated fish counts from the processing algorithm.

We demonstrate the efficacy of this method by applying it to a six-month hydroacoustic dataset collected in the tidal region of the Penobscot River, Maine USA. It enabled us to recover 60% of the data that would otherwise have been lost due to noise contamination. The successful implementation of this method allows for datasets with varying signal-to-noise ratios to be standardized based on the noise signature present, enabling researchers to maximize their data usage.

Quantifying how fish abundance changes after a significant portion of their natural habitat becomes re-accessible is critical to gauge the success of large restoration efforts. Because fish abundance also changes with naturally fluctuating environmental conditions, examining abundance relative to these conditions can indicate fish responses to both anthropogenic and natural river variation. A side-looking hydroacoustic system was used to estimate fish abundance in the Penobscot River, ME from 2010-2016, where 2010-2013 were pre-dam removal conditions, and 2014-2016 were post-dam removal conditions. The river was monitored during non-ice condition periods, roughly May to November annually. Automated data processing enabled continuous abundance estimates from fish tracks. A fourfold increase in median fish abundance occurred in the fall compared to spring and summer, regardless of dam presence. Concurrent with restoration activities, fish abundance increased approximately twofold pre- to post-dam removal. We examined the influence of natural environmental conditions including tide, discharge, temperature, diurnal cycle, day length, moon phase, as well as restoration activities (focusing on dam presence) on variability in fish abundance. Day length (or photoperiod) was the most important predictor variable in all eight time-series analyzed. During the fall migration, abundance was generally higher during outgoing tides, at night, and during

relatively high river discharge. In the early fall, when daylength was between 11.28 h and 12 h (September 24th to October 6th) and water temperature was above 11.96 °C, an eightfold increase in fish abundance was recorded in post-dam removal years. Alewife stocking numbers increased post-dam removal relative to pre-dam removal years and likely contributed to the increased fish abundance. This is one of the first validated tools to continuously examine the response of fish abundance to a major river restoration activity. In this application, it significantly increased our understanding of how fish abundance changed in the Penobscot River as result of major restoration efforts and provides a basic understanding of fish responses to naturally fluctuating environmental conditions.

ACKNOWLEDGEMENTS

I would like to thank my advisory committee, Drs. Gayle Zydlewski, Damian Brady, and Neal Pettigrew for their advice of support in my Master's studies. I especially want to thank Dr. Gayle Zydlewski for her unwavering dedication to not only bring this project to completion, but also in providing an educational experience that helped me grow both personally and professionally. I also want to thank my colleagues Haley Viehman, Aurélie Daroux, Garrett Staines, Kevin Lachapelle, Catherine Johnston, Jahnita DeMoranville, Rachel Kocik, Adam Desjardins, and James McCleave who both directly and indirectly contributed to the success of this project.

I thank Waterfront Marina in Hampden, Maine for offering access and power to the study site. This work was supported in part by an award from the National Oceanic and Atmospheric Administration (award #NA14NMF4630256), The Nature Conservancy, University of Maine School of Marine Sciences, and the Maine Agricultural and Forest Experiment Station. The views expressed herein are those of the author(s) and do not necessarily reflect the views of the Penobscot River Restoration Trust, the National Oceanic and Atmospheric Administration or any of their Members or sub-agencies.

TABLE OF CONTENTS

ACKNOWLEDGEMENTS ii

LIST OF TABLES vi

LIST OF FIGURES vii

CHAPTER 1: PROCESSING METHODS TO MAXIMIZE HYDROACOUSTIC
SAMPLING RANGE AND MINIMIZE MIDFIELD BEAM CONTAMINATION IN
DYNAMIC SYSTEMS 1

 Abstract 1

 Introduction 2

 Study site and data used..... 6

 Methods 8

 Sampling range limitations 11

 Identifying maximum range sampled 13

 Midfield beam interferences 17

 Fish counts 19

 Algorithm validation..... 19

 Fish abundance estimation..... 21

 Results 22

 Maximum range sampled 22

 Midfield beam interferences 23

 Algorithm validation..... 24

Standardized fish counts	26
Discussion	28
References, Chapter 1	33
CHAPTER 2: USING HYDROACOUSTICS TO RELATE FLUCTUATIONS IN FISH ABUNDANCE TO RIVER RESTORATION EFFORTS AND ENVIRONMENTAL CONDITIONS IN THE PENOBSCOT RIVER, MAINE.....	38
Abstract	38
Introduction	39
Methods.....	44
Sampling procedure.....	44
Data quality assessment.....	47
Automated data processing.....	50
Data correction for range.....	51
Data Analysis.....	53
Results	57
Automated processing validation	57
Range standardization.....	59
Fish abundance pre- and post-dam removal	60
Fish abundance and the environment	64
Discussion	68

References, Chapter 2	75
BIBLIOGRAPHY	82
BIOGRAPHY OF THE AUTHOR.....	89

LIST OF TABLES

Table 1.1	Echoview [®] acoustic data processing parameters	10
Table 2.1	Annual dates for side-looking deployment of BioSonics split beam transducers in the Penobscot River, Maine.....	46
Table 2.2	Relative data quality of archived side-looking hydroacoustics data collected in the Penobscot River, ME.....	48
Table 2.3	Numeric values representative of different environmental variable conditions assigned to each sampling hour and used in CART analysis.....	55
Table 2.4	Median fish abundance (fish h ⁻¹ m ⁻¹) and sampling range (m) broken down by year and river side.....	64
Table 2.5	Relative variable importance identified by the CART model with the highest relative predictability.....	66

LIST OF FIGURES

Figure 1.1	River surface reflectance causing variable ranges of usable data in an acoustic echogram.....	5
Figure 1.2	Map of the Penobscot watershed in Maine and the relative location of the study site	7
Figure 1.3	Simplified cross-sectional illustration of the experimental setup at the survey sites in the Penobscot River, ME.....	8
Figure 1.4	Interference sources limiting the maximum sampling range during low and high tide.....	12
Figure 1.5	Example of cell grid implementation to identify regions of high noise contamination	16
Figure 1.6	Tidal height of the Penobscot River and the corresponding maximum sampling range of the transducer.....	22
Figure 1.7	Beam masked percentages (grey zones) by tidal stage.....	23
Figure 1.8	Regression plot between automated fish counts and manual counts used for algorithm validation.....	24
Figure 1.9	Difference between automated and manual counts for different resample percentages used in the processing algorithm	25
Figure 1.10	Sensitivity analysis for the number of files used for comparing manual and automated fish counts	26
Figure 1.11	Mean, median, and mode for the maximum range line from a random data collection day in 2015	27

Figure 1.12	Time series of fish counts binned by hour across six months sampled in 2015	28
Figure 2.1	Cross-sectional illustration of the experimental setup at the survey sites in the Penobscot River	45
Figure 2.2	Map of Penobscot watershed in Maine and relative location of the study site	47
Figure 2.3	Histogram of all fish tracks detected by range.....	52
Figure 2.4	Regression plots of automated and manual fish counts for each year and river side sampled in the Penobscot River, ME	58
Figure 2.5	Fish h^{-1} metric (A) and fish $h^{-1} m^{-1}$ (B) metric compared by range sampled	59
Figure 2.6	Fish tracks sampled within the first 15 meters of the transducer beam for all years pre- and post-dam removal.....	60
Figure 2.7	Fish abundance pre-and post-dam removal grouped by season.....	61
Figure 2.8	Recorded fish abundances (fish $h^{-1} m^{-1}$) in the Penobscot River for each year and river side sampled from 2010-2016	63
Figure 2.9	Pruned decision tree created by CART analysis with a total of 21 nodes	68

CHAPTER 1:
PROCESSING METHODS TO MAXIMIZE HYDROACOUSTIC SAMPLING
RANGE AND MINIMIZE MIDFIELD BEAM CONTAMINATION
IN DYNAMIC SYSTEMS

ABSTRACT

Spatiotemporal advantages linked to hydroacoustic sampling techniques have caused a surge in the use of these techniques for fisheries monitoring studies applied over long periods of time in marine systems. Dynamic physical conditions such as tidal height, boat traffic, floating debris, and suspended particle concentrations result in unwanted noise signatures that vary in intensity and location within a hydroacoustic beam over time and can be mixed with the acoustic returns from intended targets (e.g., fish). Typical processing filters applied over long term datasets to minimize noise and maximize signals do not address spatiotemporal fluctuations of noise in dynamic systems. We present a methodological approach to obtain fish counts from large hydroacoustic datasets collected in dynamic systems by 1) developing an automated processing algorithm that imposes spatially and temporally varying noise thresholds according to the signal-to-noise ratio present, 2) creating a fish count index standardized to the noise conditions present at the time of detection, and 3) validating the applied algorithm by manually quantifying the margins of error of automated fish counts from the processing algorithm. We demonstrate the efficacy of this method by applying it to a six-month hydroacoustic dataset collected in the tidal region of the Penobscot River, Maine USA. It enabled us to

recover 60% of the data that would otherwise have been lost due to noise contamination. The successful implementation of this method allows for datasets with varying signal-to-noise ratios to be standardized based on the noise signature present. This provides the opportunity for researchers to maximize their data usage by not having to restrict their dataset to a common divisor in data range and quality.

INTRODUCTION

Hydroacoustic technology has become increasingly popular for scientific studies involving fish abundance estimates (Hughes and Hightower, 2014; Auer and Baker 2007; Simmonds and MacLennan, 2005) and other ecosystem features such as tidal fish migrations (Krumme, 2004), deep-sea krill swimming behavior (Klevjer and Kaartvedt, 2003), abundance estimates of squid (Zhang *et al.*, 2015), and small scale oceanographic features such as zooplankton biomass estimates (Ballón *et al.*, 2011). Hydroacoustic survey methods have multiple benefits compared to traditional fish survey methods, which make them more advantageous for answering specific abundance questions. With hydroacoustic applications, abundance estimates can be made over large temporal and spatial scales, which can be used for ecosystem-based fisheries management (Koslow, 2009; Trenkel *et al.*, 2011) and species-specific fish population studies (Daum and Osborne, 1998). Specific applications also include studies in habitats as diverse as lakes and open sea mesopelagic zones: e.g., fish recruitment indices for walleye pollock (*Theragra chalcogramma*) in the Bering sea (Swartzman *et al.*, 1995); northern lantern fish (*Benthoosema glaciale*) and Mueller's pearlside (*Maurolicus muelleri*) (Scouling *et*

al., 2015) populations in the Norwegian Sea; schooling of herring (*Clupea harengus*) and mackerel (*Scomber scombrus*) (Misund and Beltestad, 1996); and predator-prey interactions between killer whales (*Orcinus orca*) and adult herring (Similä, 1997).

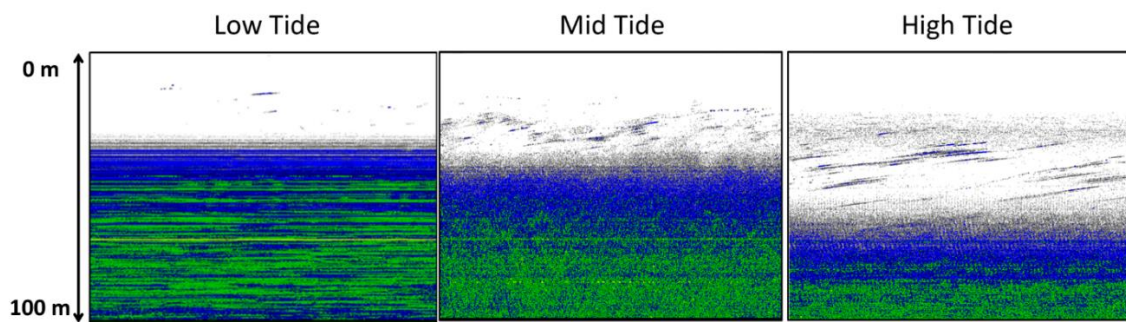
In hydroacoustic studies, data quality can be limited considering that the intended targets (e.g., fish) are not the only acoustic returns recorded by the equipment used (Mann *et al.*, 2008). Data quality can be quantified as the ratio of acoustic signal strengths of the fish targets with any other acoustic targets recorded (Kieser *et al.*, 2005). Every target ensonified by the acoustic beam has a specific back scattering signature recorded as target strength (TS) (Love, 1977). The TS returns from fish are different from other sound reflecting targets. Reflections other than from fish are considered “noise” to the fish biologist but could be counted as false fish signals if not adequately minimized or removed in data processing (Banneheka *et al.*, 1995). If fish targets are clearly distinguishable from the surrounding noise, the data is classified as having a good signal-to-noise ratio (SNR) (Kieser *et al.*, 2005). Fish targets can be isolated from surrounding noise using processing programs, e.g., Echoview[®] (Fraser *et al.*, 2017; Viehman *et al.*, 2015; De Robertis and Higginbottom, 2007) or SONAR5 (Samedy *et al.*, 2015). Algorithms established in these programs are used to remove noise sources from datasets that otherwise would falsely be counted as fish. Constant noise sources, such as a stationary rock in the acoustic beam, are easily removed with such algorithms because the position and TS of the rock does not change over time. In addition, interference sources can have a consistently higher TS value than the fish targets and are easily removed by applying a TS threshold. However, when the TS and the location of the noise source in the acoustic beam varies over time, standard algorithm noise removal filters must be

modified to adjust to the changing noise levels. Spatiotemporally varying noise levels in a dataset may then cause the sampling range of data with acceptable SNR to fluctuate based on where in the beam these interferences occur. This can then have a profound effect on data quality and its interpretation as fish abundance estimates.

Hydroacoustic data are now more frequently being collected at study sites in dynamic aquatic systems that experience changing physical conditions (Fraser *et al.*, 2017; Viehman *et al.*, 2015; Samedy *et al.*, 2015). Such conditions result in changing noise levels over time, which cause the range of acceptable data quality sampled by the transducer to also vary over time (i.e., varying sampling range). Thus, data that are compared across temporal dimensions must be standardized in space. In horizontally oriented (side-looking) hydroacoustic systems in tidal rivers, for example, sound can be reflected from the surface at different distances from the transducer as the water level changes with the tide. This results in temporally varying noise levels that change spatially (Figure 1.1). The maximum range sampled by the hydroacoustic system is decreased when the acoustic beam encounters the river surface at a closer range during low tide, and increased during high tide. An increased sampling range yields an increased probability for capturing fish signals, as more water is sampled where fish might be present. When comparing two fish abundance data points collected at different times and with different maximum sampling ranges, it is necessary to standardize both data points by their respective sampling ranges for the comparison to be valid. This is similar to other standardization techniques in the field of fisheries including the application of catch per unit effort (CPUE) to standardize the number of fish captured over units of time, tows, vessels, and area (Bentley *et al.*, 2010).

Other sporadic noise sources also affect data quality. High particle concentrations in the water column after storm events, surface waves from wind and boat traffic, intermittent debris floating through the acoustic beam, and other natural river conditions reduce the midfield beam quality, thus degrading SNR and the ability to isolate fish from other objects in the acoustic beam (Rudstam *et al.*, 2008). These sporadic noise intensive sources are at risk of being counted as multiple fish targets. Noise contaminants become especially difficult to eliminate if they are present in the middle of the acoustic beam pattern. We addressed this scenario along with changing spatial range, where hydroacoustic data quality is dictated by the dynamic processes occurring within the aquatic system sampled.

Figure 1.1. River surface reflectance causing variable ranges of usable data in an acoustic echogram. Data collection range and quality were highly dependent on the tides.



Hydroacoustic systems can collect multiple data points per second (Trenkel *et al.*, 2011). As such, long term deployments make the collection of large datasets possible, yet difficult to process. The sheer quantity of data collected will often make manual processing nearly impossible, especially with limited resources in time and personnel.

Automated processing methods developed for adapting to the changing noise level and sampling range conditions could enable temporally comparable, spatially standardized fish counts.

We present automated processing methods that produce accurate estimates of fish numbers by reducing spatiotemporally varying noise contamination. We also illustrate how fish estimates were standardized in an abundance index that makes it possible for them to be compared to other, temporally different datasets with independent noise signatures. The methods described in this paper should be useful to researchers experiencing temporally varying sampling volumes and midfield noise contamination in hydroacoustic data.

Study site and data used

The methods described in this paper were developed by processing and analyzing hydroacoustic data collected for a fish abundance monitoring program in the upper reaches of the Penobscot River estuary in Maine, USA. This monitoring program was part of the Penobscot River Restoration Project (PRRP). The study site was located 5 km downstream from the city of Bangor (Figure 1.2). Stationary hydroacoustic survey systems were installed to monitor fish abundances in the river from a pre-dam removal to a post-dam removal condition. One 206 kHz transducer was deployed in a side-looking orientation on each side of the river sampling at four pings per second. Each transducer projected an acoustic beam across the river (Figure 1.3). Data collection began in 2010 and continued through 2016, but was only possible from May to approximately November of each year due to drifting ice blocks in the river during winter that could

damage the equipment. The river was 195 m wide at the study side with a median channel depth of 7 m and a tidal range of up to 5.25 m. Each transducer was installed to be approximately 2 m below the river surface during low spring tide. The Penobscot River experienced a discharge ranging from $100 \text{ m}^3\text{s}^{-1}$ to $2000 \text{ m}^3\text{s}^{-1}$ between May and December of 2015 with peak flows occurring in early October (USGS station 01036390 Penobscot River at Eddington).

Figure 1.2. Map of the Penobscot watershed in Maine and the relative location of the study site. (A) the Penobscot watershed in Maine, (b) the relative location of the study site by river km, and (c) the approximate locations of the acoustic beams; Pen A and Pen B are the west and east side locations of annual transducer deployments.

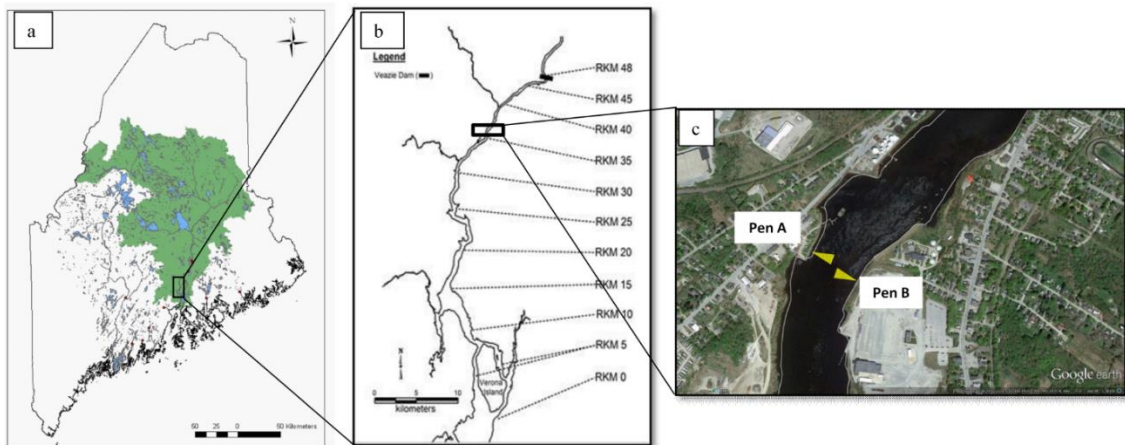
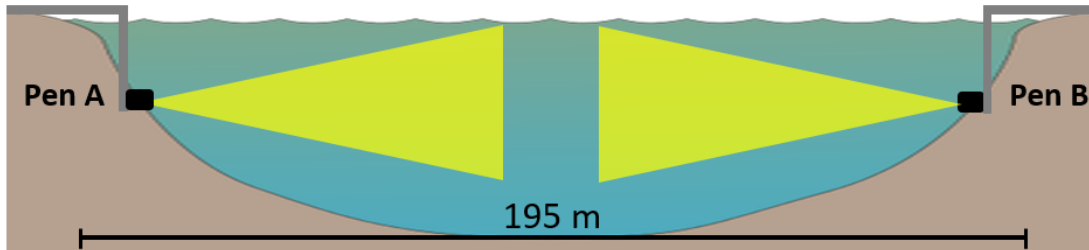


Figure 1.3. Simplified cross-sectional illustration of the experimental setup at the survey sites in the Penobscot River, ME.



The objective of this hydroacoustic monitoring study was to compile a relative fish abundance index for each year sampled, where the pre-dam removal years could then be compared to post-dam removal years. For this paper, we focused on a specific six-month subset of data from 2015 collected on the Pen A river side (Figure 1.3) to illustrate individual processing steps and demonstrate the validity of the approach. Ultimately, this data-processing approach will be used on four, six-month hydroacoustic datasets collected on the Penobscot River to generate and compare fish abundance indices pre-and post-dam removal.

METHODS

Processing methods in this paper were built on the cell-based noise removal method of De Robertis and Higginbottom (2007). In addition, we (a) applied an alternate noise removal procedure for the midfield beam region in the TS domain, and (b) implemented a noise-varying maximum range line that addresses a changing volume sampled over time.

The parameter values used in the processing algorithm created in Echoview[®] were specifically identified for the dataset collected from May to December on the Pen A river side in 2015 (Table 1.1). The specific parameter values presented in Table 1.1 are subject to change when processing different datasets. However, the methodological approach of how to minimize range varying noise contamination is applicable for different datasets experiencing similar conditions. While additional variables were used in the final algorithm applied to these data, the variables listed in Table 1.1 reflect the core parameters of the algorithm's maximum range detection and overall noise removal approach.

Table 1.1. Echoview® acoustic data processing parameters.

<i>Variable</i>	<i>Parameter/ Variable</i>	<i>Value</i>
<i>Single target detection: single beam method 2</i>	TS threshold	-45 dB
	Pulse length determination levels	6, 12, 18 dB
	Min. normalized pulse length	0.30, 0.60, 0.80
	Max. normalized pulse length	3.00, 2.10, 5.00
<i>Fish tracking: 2D</i>	Data	2D
	Alpha (range)	0.1
	Beta (range)	0.1
	Exclusion distance (range)	0.4 m
	Missed ping expansion (range)	0.8 %
	Weights:	
	Range	0.00
	TS	0.00
	Ping gap	0.00
	Min. number of single targets in a track	6
	Min. number of pings in a track (pings)	6
	Max. gap between single targets (pings)	12
<i>Resample (by number of pings)</i>	Min. threshold (Data)	-49 dB
	Ping selection:	All pings in interval
	Number of pings in interval (m)	300
	Resampling operation:	Percentile
	Percentile	70.00
	Number of data points (n)	50
<i>Best Candidate Line Pick</i>	Start depth (m)	0.00
	Stop depth (m)	1000
	Minimum Sv for good pick (dB)	-100
	Discrimination level (dB)	-100
	Backstep range (m)	-0.50
	Peak threshold (dB)	-50.00
	Maximum dropouts (samples)	2
	Window radius (samples)	8
Minimum peak asymmetry	-1.00	
<i>Data Range Bitmap</i>	Minimum in-range data value	12.00
	Maximum in-range data value	100.00

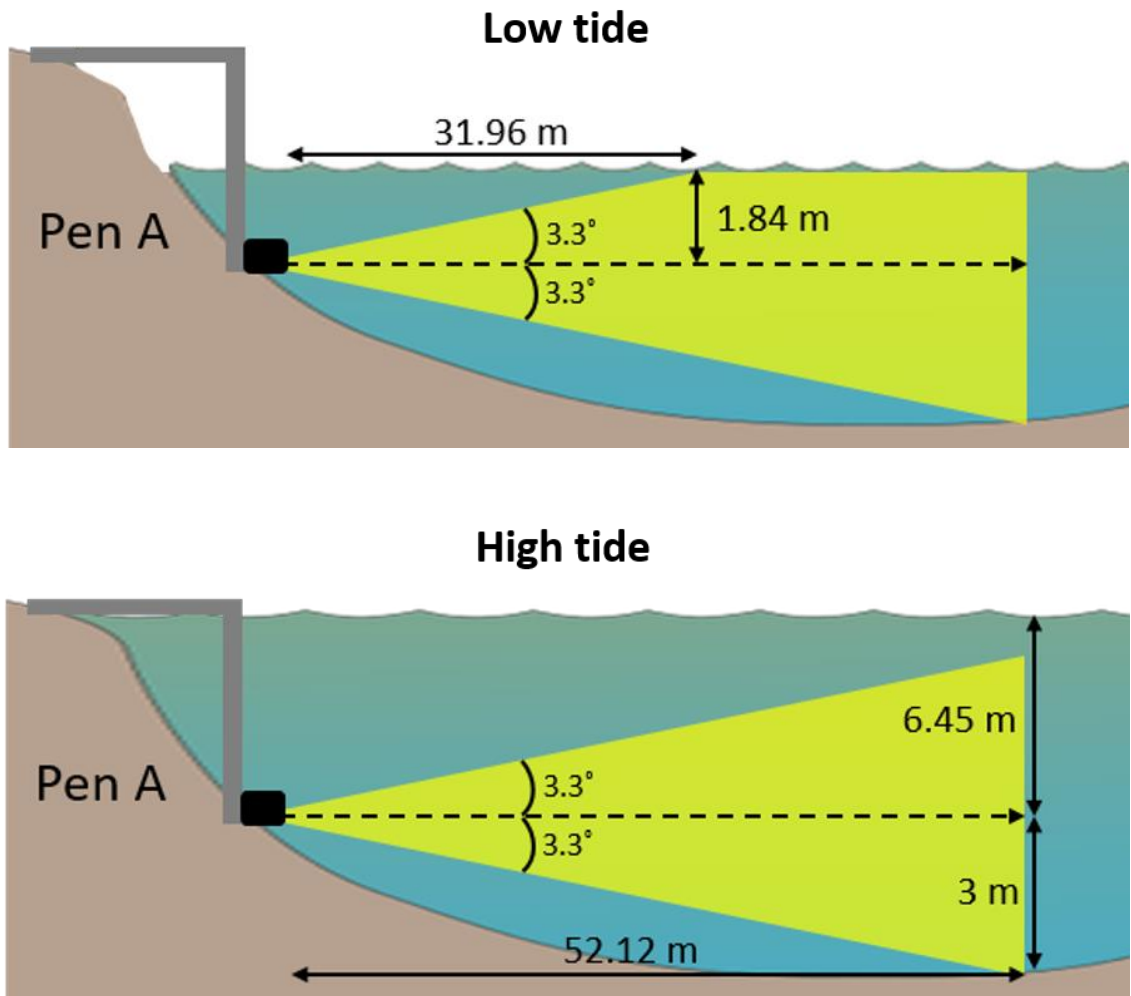
Sampling range limitations

A 206 kHz transducer was deployed in 2015 on the Pen A river side with a circular 6.6° beam angle. It was installed in a side-looking orientation below the river surface with an average depth of 1.84 m during low tide, and 6.45 m during high tide.

The transducer was positioned 3 m above the river bottom measured 60 m from the transducer. Interference sources appearing at a sampling range of approximately 30 m during low tide and 60 m during high tide (Figure 1.1) were linked to the acoustic beam encountering either the river bottom or river surface during different tidal stages.

Trigonometric calculations confirmed that during low tide noise reflections from the river surface would limit the sampling range to approximately 32 m, while at high tide the river bottom limited the sampling range to approximately 52 m (Figure 1.4). These calculations assume a perfectly balanced horizontal, side-looking aim of the transducer, which was presumptuously not the case in reality. Margins of error of ± 9 m in the theoretical sampling range at high and low tide are to be expected based on the actual aim of the transducer not being perfectly horizontal (based on $\pm 0.5^\circ$ angle errors).

Figure 1.4. Interference sources limiting the maximum sampling range during low and high tide. Theoretical sampling ranges at which we expect to see noise interferences in the data at low tide (31.96 m) and high tide (52.12 m). The expected ranges are consistent with the observed interference ranges in Figure 1.1.



Identifying maximum range sampled

The issue of a tidally influenced sampling range was addressed by implementing a variable maximum range line that was set relative to the range at which the transducer beam encountered the river surface. To do this, the echogram was condensed into an n by m sized cell grid (Table 1.1) according to the equations of the Echoview[®] *resample* variable:

$$R_{i,j} = \frac{r_{i,j+1} + r_{i,j}}{2} \quad \text{for } j = 1 \text{ to } n-1$$

$$D_{i,j} = \frac{d_{i,j+1} + d_{i,j}}{2} \quad \text{for } i = 1 \text{ to } m-1$$

where i is the ping number, j the index for vertical samples of each ping in the echogram, $R_{i,j}$ is the near range boundary (m) of sample j in ping i of the echogram, $D_{i,j}$ is the near boundary distance (n) of ping i for sample j in the echogram, $r_{i,j}$ is the range of sample j in ping i of the echogram, and $d_{i,j}$ is the distance of ping i for sample j in the echogram.

The adaptability of the maximum range line to the noise reflected from the river surface was limited by the cell size specified in the *resample* variable in Echoview[®] (Table 1.1). As such, the spatiotemporal unit of one cell represented the smallest interval at which the maximum range line could vary. The n domain of the cell grid used for data processing consisted of 300 horizontal pings as its x statistic (representative of time), and 50 vertical regions as its y statistic (representative of space) as its m domain. At a sampling rate of four pings per second and a transducer beam range of 100 m, the size of each cell consisted of a spatiotemporal unit of 75 seconds (n) by 2 m (m). This meant that the maximum range line could adjust to changing noise levels in the river every 75

seconds by at least 2 m at its minimum, as this is the size of one cell. However, the maximum range line would only adjust if the noise level within a cell exceeded a specified threshold.

To determine the noise level in each cell, a TS value representative of the seventieth percentile of all TS values within each cell was calculated. The seventieth percentile was identified to be suitable using the algorithm validation procedure, as it proved to be the most successful at removing noise contamination across all tidal stages while maintaining fish targets (see *Algorithm Validation* section). The calculated TS value was then assigned to the entire cell as:

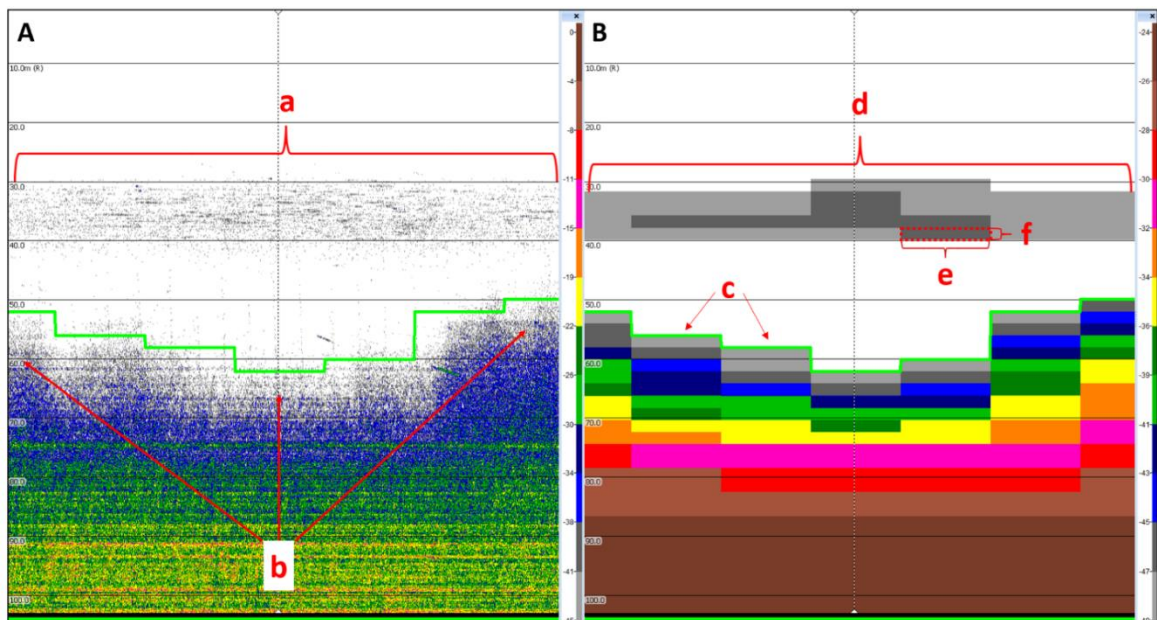
$$y_{I,J} = W_k + (W_{k+1} - W_k)(k' - k)$$

where $y_{I,J}$ is the value of sample J in the output ping I , W_k is the TS value of sample k in the list W , W is the ordered list of sample values $x_{i,j}$ for all i,j in set Y , such that $W_i \leq W_{i+1}$, $k' = N * P$, $k = [k']$, N is the number of samples in W , P is the desired percentile to be calculated.

Once the cell's TS values were established, Echoview[®]'s *Best Candidate Line Pick* variable was used to set the maximum range line on the nearside boundary of each cell with a TS value exceeding a threshold of -49 dB (Figure 1.5B c). This threshold was representative of a minimum noise level above which fish were difficult to isolate without risking false classification. If the noise level changed in range over time, such as when the acoustic beam encountered the surface of the river, the TS value of the local cells would change accordingly. This then caused the maximum range line to adjust to the range of the cell where the TS value exceeded the specified threshold of -49 TS

(Figure 1.5B). Throughout, a variable maximum range line was created that automatically adjusted to the range at which the acoustic beam encountered the river surface, enabling us to use the most possible data sampled across all tidal stages. Data within the maximum range line was further processed for noise reduction and fish classification.

Figure 1.5. Example of cell grid implementation to identify regions of high noise contamination. Displayed is a raw TS echogram (A) and its corresponding cell grid implementation (B) to identify regions of high noise contamination. Midfield beam contamination (a) and variable sampling ranges of usable data (b) are evident. Noise signatures of each cell are used to create a flexible maximum range line (c) and to minimize the effects of midfield beam interferences through grey zones (d), where each cell represents a spatiotemporal unit of 300 pings in the n domain (e), and 2 m in the m domain (f). The color spectrum corresponds to the relative target strength of the returned acoustic signal, where strong returns are illustrated in brown (-24 dB and above) and the weakest signals admitted for processing are shown in grey (-49 dB).



The described cell grid size was chosen as a compromise, as a larger grid size would have resulted in lower flexibility of the set maximum range line, and a smaller grid size would run the risk of masking out small schools of fish if they filled the entire

spatiotemporal unit of one cell. The cell grid was applied for the entire six-month dataset and used to identify the maximum range sampled as well as contend with midfield beam interferences.

Midfield beam interferences

Data quality varied with range. Data collected during high and mid tide periods often experienced midfield beam interferences at increased sampling ranges. The source of midfield beam interferences was assumed to be the result of side-lobe beam(s) encountering the river bottom at a range of approximately 30 m. As the sampling range of the main lobe (i.e. main beam) encounters the river surface at about the same distance, the midfield beam interference caused by the side-lobe is masked by the interferences caused by the river surface. Once the river depth increases and the main beam extends past the distance at which the side-lobe interference occurs, the midfield beam interference is again visible. During these times, the signal-to-noise ratios were high in the near-field, low in the midfield ranges, and high again in the far-field beam regions (Figure 1.5A). The algorithm was customized to mask the varying noise level intensities experienced in the midfield beam region, enabling the full range of the acoustic beam to be used for fish target classification. This was achieved by identifying acoustic beam regions that were contaminated with noise. These midfield noise zones, “grey zones,” were subject to stricter fish target isolation procedures than the non-contaminated-beam regions to avoid false fish classifications. Grey zones were identified using the same m by n cell grid as for the maximum range line (Figure 1.5B). All cells were assigned one TS value that was representative of the 70th percentile of all TS values within the cell. If the

assigned TS value of a cell exceeded the -49 TS threshold, they were classified as grey zones, but only if the cell range was located before the maximum range line. Cells past the maximum range line were ignored. Grey zones were subject to a masking filter in form of a *Data Range Bitmap* (Table 1.1) that required TS values within the grey zone cells to be at least 12 dB higher than the TS value assigned to the cell to be quantified as a target instead of noise. As such, fish could still be counted in the noise contaminated regions of the acoustic beam classified as grey zones, given that their TS value was at least 12 dB above the noise surrounding them.

Because the minimum TS threshold for fish located in grey zones was higher than those for the remaining, uncontaminated beam regions, an analysis of the total beam percentage masked for each tidal stage was performed. Tidal stage was analogous to the range sampled and used as a category to group files with similar sampling ranges. We estimated what percentage of the beam area was subject to midfield noise and thus higher fish count restrictions for each tidal stage. Hydroacoustic data files were sorted into tidal stage bins by matching the data collection times to a water depth time series recorded by a HOBO depth recorder deployed on the transducer mount. The HOBO depth tag was installed 1.21 m above the actual transducer connected to the mount. Because the change in river depth at the transducer (i.e., tidal height) spanned approximately 5.25 m, bins were divided into 0.25 m intervals, which was the average change in water depth during one 15-min hydroacoustic file. With a tidal range of 5.25 m at the study site, this resulted in a total of 21 tidal stage bins based on depth. Ten 15-min files were randomly selected from each tidal stage bin, and the number of masked and unmasked cells were exported

as binary values to a *.csv* file. The exported binary values were used to calculate the beam percentage masked for each tidal stage.

Fish counts

Fish counts were obtained by applying Echoview[®]'s fish tracking algorithm to the fish targets remaining after all noise removal and isolation procedures had been concluded. Potential fish targets were further isolated from any remaining noise by setting acceptable fish target criteria. To be counted as a fish target, a returned ping had to pass pulse length thresholds implemented at 6 dB, 12 dB, and 18 dB. The thresholds implemented at these pulse lengths were specific to the collection properties of the transducer used and determined by inspecting the pulse length determination values from a likely fish target in the acoustic beam. The appropriate thresholds at each pulse length interval were evaluated based on manual observations through trial and error (Table 1.1). The Echoview[®] fish tracking parameters were optimized according to the results of the algorithm validation procedure (Table 1.1) (see *Algorithm Validation*).

Algorithm validation

The validity of the algorithm applied to obtain fish counts was examined. A subsample of 90 data files composed of 30 files collected during *high*, *mid*, and *low* tides were randomly chosen from the full dataset of approximately 15,000 files. Each file of the subsample represented 15 minutes of acoustic data and was visually inspected for fish tracks in the raw TS echogram. At least three people experienced with hydroacoustic data

counted the numbers of fish in each of the 90 files. To maintain consistency among counters in fish classification and counting procedures, files were recounted if fish counts per file deviated by more than 5% among counters. All 90 files were then processed with the established algorithm in Echoview®.

The sums of all fish counted manually and by the algorithm were compared for the 90 files. A regression analysis was performed, where the algorithm was deemed successful if the r-squared values for files of each tidal stage was greater than 0.8. If the algorithm values were below 0.8, the automated counts either represented an over- or under estimation of fish compared to the manual counts. In this case, the parameter values described in Table 1.1 were revised based on the differential between manual and automated counts.

The final algorithm used for processing was a product of all variables set with parameter values that exhibited the lowest differential between manual and automated counts. An example of this approach is demonstrated for the *resample percentile* parameter, as it was the most decisive variable for the background noise removal calculations and had the largest impact on the number of fish counted by the algorithm. To determine which *percentile* would be most appropriate for noise removal and fish target retention, an independent iteration of the algorithm was performed in ten *percentile* increments on the 90-file data subsample. The *percentile* used ranged from 10 to 100 and increased by 10 for each iteration. To determine which percentile would yield the most accurate fish counts in the algorithm, the difference between manual fish counts and automated counts was used. The most accurate percentile would represent the smallest deviations from 0 for each of the 90 files processed.

A sensitivity analysis was also performed to determine if 90 files, 30 from each tidal stage, was an appropriate number of files to use for the algorithm's validation procedure. If the r-squared values from a correlation between automated and manual counts only experienced negligible variations by adding additional files to the regression analysis, it can be concluded that the number of files, after which little variation in the R^2 value occurs, would be a sufficient representation of the entire dataset.

Fish abundance estimation

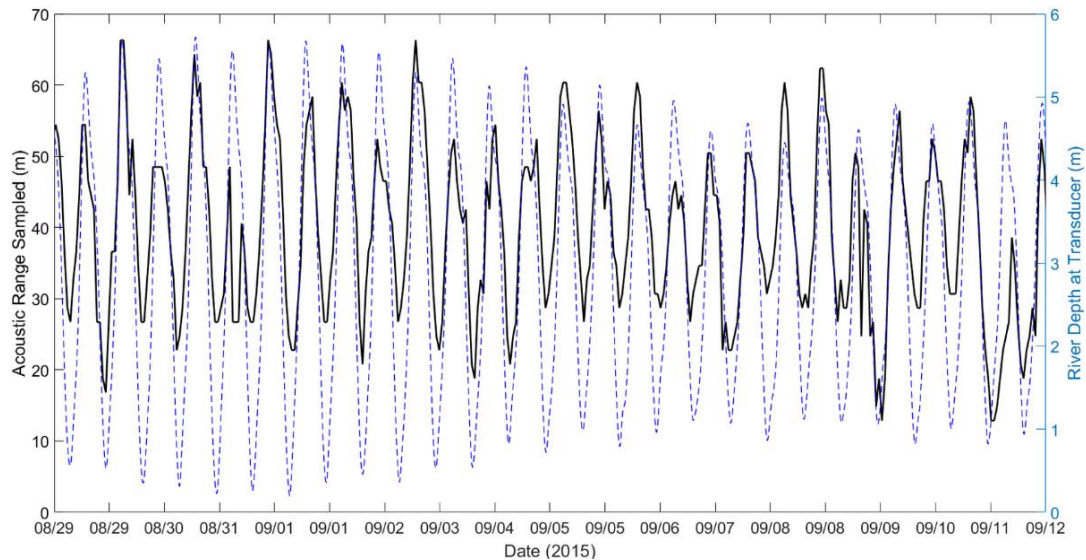
Fish abundance estimates were compiled from the fish counts obtained by Echoview[®]'s fish tracking procedure, where one fish track equaled one fish count. To create an index that allowed fish abundance comparisons over time, the number of fish counted over time was standardized by the range sampled. One 15-min file was uploaded at a time to the Echoview[®] template file containing the data processing algorithm. Once processed, the maximum range line for each individual ping and information about the fish tracks present were exported as .csv files for each 15-min hydroacoustic file. Visual Basic Scripting (VBS) was used to automate these steps for the entire continuous dataset spanning approximately 6 months. The .csv files were uploaded to MATLAB to calculate the median range sampled per hour and bin the number of fish tracks by hour for the entire collection period. Total numbers of fish per hour were then divided by the corresponding median range sampled for that hour to create the final metric used for comparing fish abundance estimates over the entire long-term dataset: fish counts hour⁻¹ meter sampled⁻¹ (fish h⁻¹ m⁻¹).

RESULTS

Maximum range sampled

Based on the noise algorithm applied to the dataset, from May 20 to December 7, 2015, the sampling range, with acceptable SNR, fluctuated between 12 m and 65 m and was reflective of the depth of the water (which fluctuated with the tide) at the sampling station in the Penobscot River (Figure 1.6). River depth at the transducer housing platform varied between 0.25 and 5.5 m.

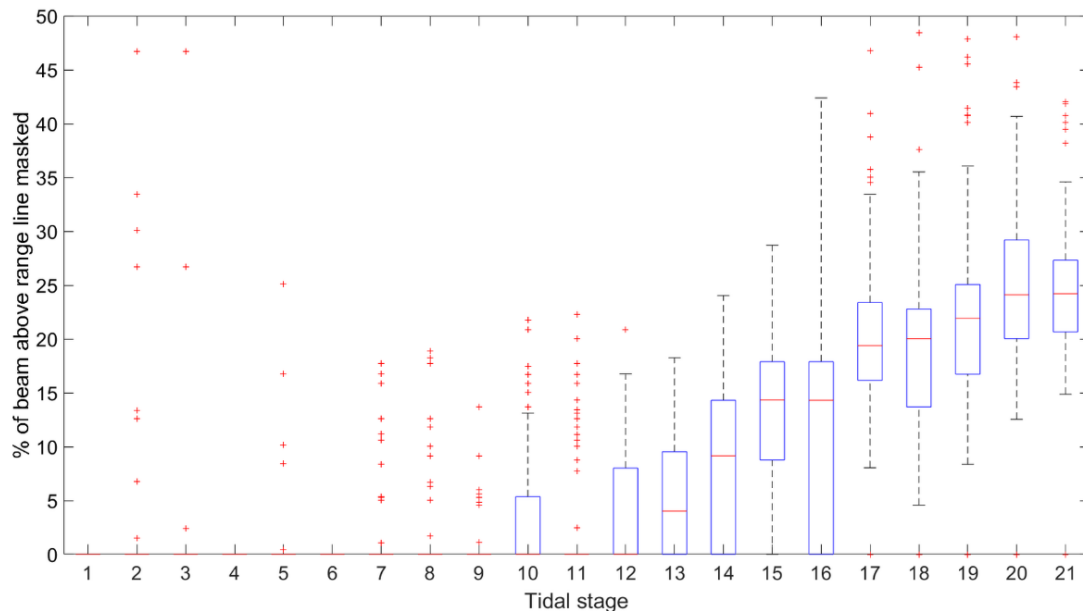
Figure 1.6. Tidal height of the Penobscot River and the corresponding maximum sampling range of the transducer. Depth the HOBO tag installed on the transducer mount (right-hand y-axis) and the maximum range sampled (left-hand y-axis) for a two-week subsample of data.



Midfield beam interferences

The percentage of the beam masked to reduce midfield beam interference was higher for longer sampling ranges that resulted due to tidal fluctuations (Figure 1.7). With a tidal range of 5.25 m at the study site, each tidal stage bin had a 0.25 m change in the water level, resulting in a total of 21 tidal stage bins. Tidal stages 1 through 7 were categorized as *low tide*, 8 to 14 as *mid tide*, and 16 to 21 as *high tide*.

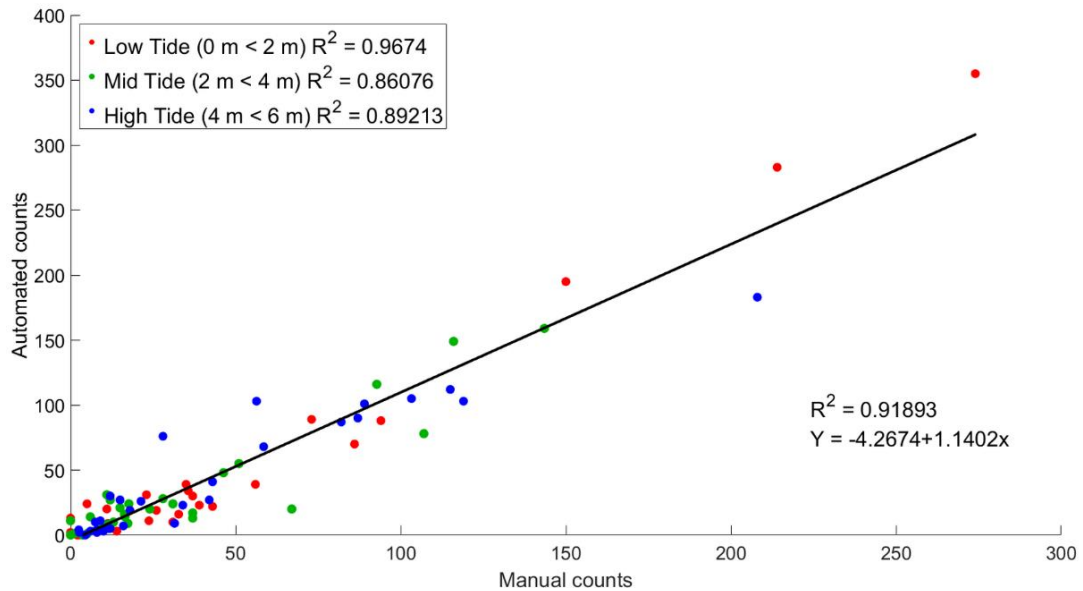
Figure 1.7. Beam masked percentages (grey zones) by tidal stage. Ten 15-min files were sampled for each tidal stage. The beam masked percentage for each ping was calculated. N = 36000. For each box plot the red central line indicates the median, the bottom and top edges the 25th and 75th percentiles, respectively, and the top and bottom whiskers the 95% confidence intervals. The red markers represent outliers.



Algorithm validation

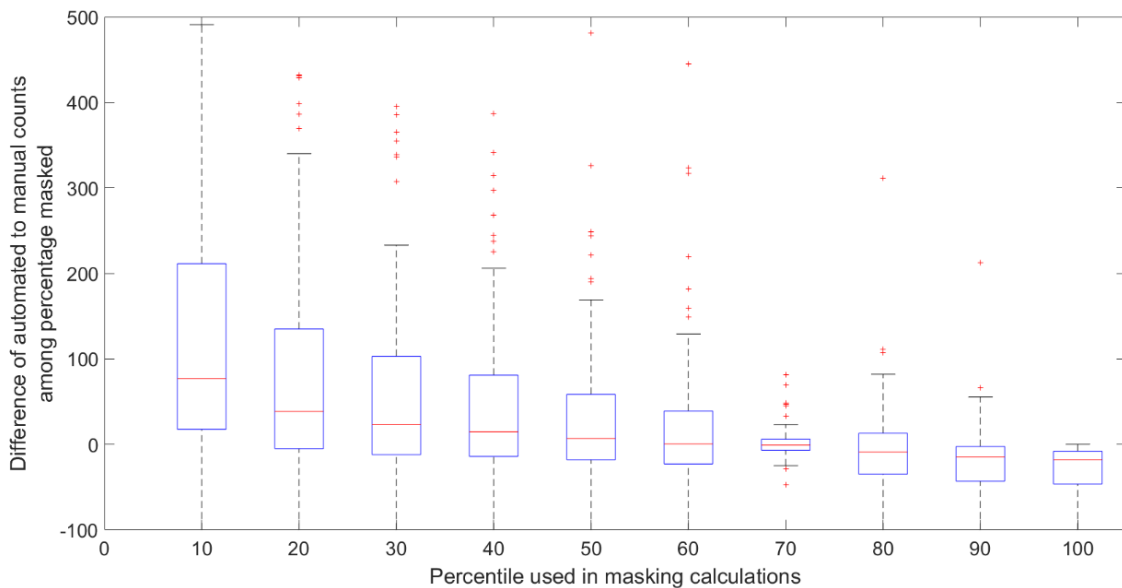
Automated and manual counts of all tidal stages were highly correlated (Figure 1.8). Low tide counts were better correlated than those during mid and high tides, but all R^2 values were at least 0.86 and the overall R^2 for all files was greater than 0.9. The slope of the relationship between manual and automated counts was larger than one, indicating a slight overestimation of fish in the automated counts for all tidal stages combined. Low tide files experienced an overestimation of 6%, high tide files an overestimation of 2%, and mid tide files an underestimation of 2%.

Figure 1.8. Regression plot between automated fish counts and manual counts used for algorithm validation. The R^2 values in the legend are from a regression for each tidal category separately (low, mid, and high). The R^2 and slope equation below the trend line represent the regression analysis for all files combined, $n = 90$.



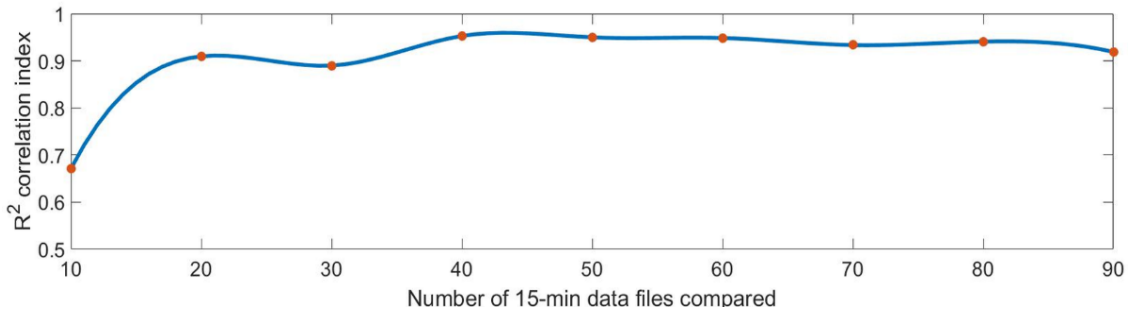
The differences between manual and automated counts had the highest variance when the percentile of the data masked was lowest. That is, the less noise masked, the less accurate the algorithm was at counting fish as some of the unmasked noise was counted as fish targets. There was a steady decrease in the difference between manual and automated count values as the percentile used for masking noise increased. The lowest variance in the difference between manual and automated counts was observed when using the 70th percentile for the *resample* variable in the algorithm for noise removal (Figure 1.9).

Figure 1.9. Difference between automated and manual counts for different resample percentages used in the processing algorithm. N = 90. Box plot definitions are described in Figure 1.7 caption.



The sensitivity analysis on the number of files needed to represent the entire dataset revealed that the correlation index between manual and automated counts remained above 0.9 at a sample size of 30 and greater (Figure 1.10).

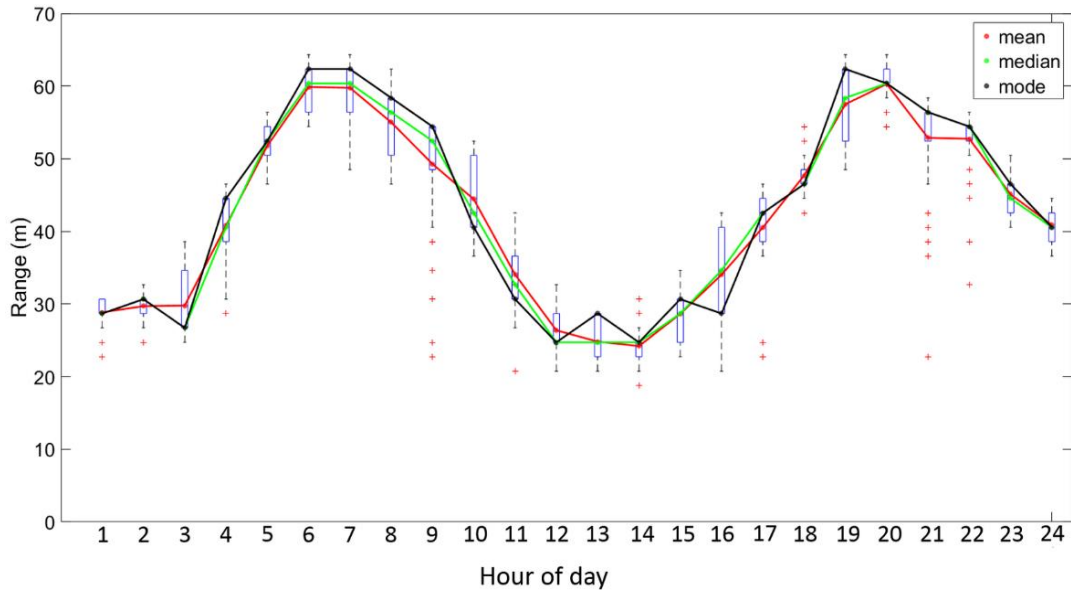
Figure 1.10. Sensitivity analysis for the number of files used for comparing manual and automated fish counts. The sensitivity analysis depicts the R^2 value for different numbers of files used in the regression analysis between automated and manual counts. Variability of R^2 values between 30 files and 90 files used in the regression analysis was <0.05 .



Standardized fish counts

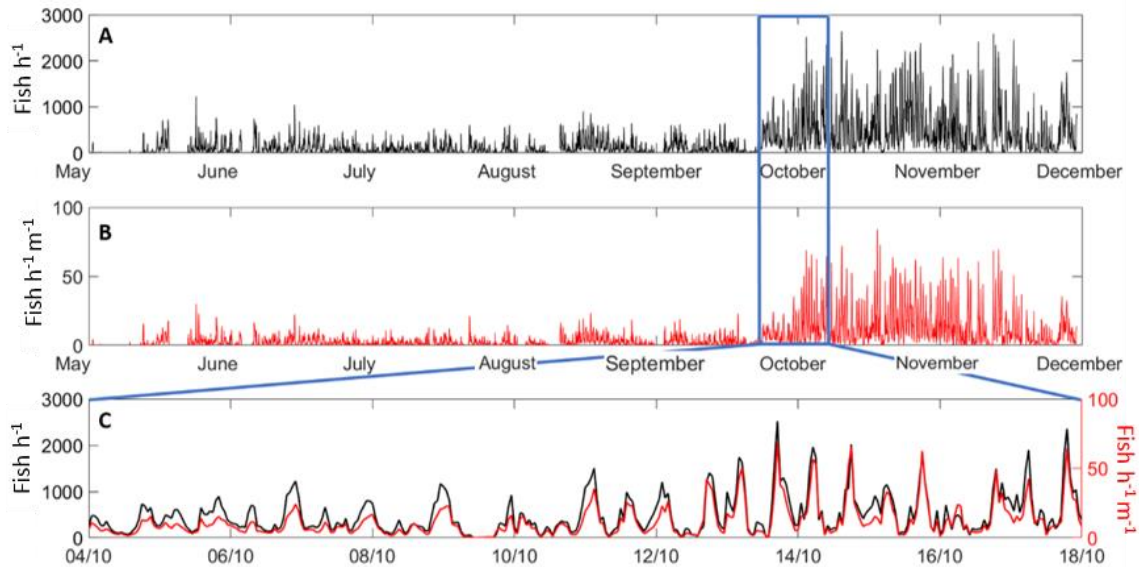
Since counts were binned in 1-hr intervals, the sampling range needed to be binned by the same time period for fish counts to be standardized by sampling range. However, multiple sample ranges existed within 1-hr bins. We explored mean, median and mode as indexing mechanisms within the 1-hr bin (Figure 1.11). The median range per hour was chosen for the standardizing unit as it minimized the effect of outliers that could be attributed to objects passing close to the beam.

Figure 1.11. Mean, median, and mode for the maximum range line from a random data collection day in 2015. Box plot definitions are described in Figure 1.7 caption.



The number of hourly binned fish counts across all six months sampled varied significantly between months (Figure 1.12A) with fish h^{-1} ranging from 0 to 2800 and fish $\text{h}^{-1} \text{m}^{-1}$ ranging from 0 to 80 (Figure 1.12B). While the general trend for both fish abundance indices remained similar, the intensity of fish h^{-1} peaks were lowered when standardized by range sampled. Variability in fish abundance from May to September fluctuated between 0 and 25 fish $\text{h}^{-1} \text{m}^{-1}$. An increase in fish abundance was observed from October to December, with fish $\text{h}^{-1} \text{m}^{-1}$ ranging from 0 to 80.

Figure 1.12. Time series of fish counts binned by hour across six months sampled in 2015. Depicted are fish h^{-1} (A), fish $\text{h}^{-1} \text{m}^{-1}$ (B), and two weeks in October with fish h^{-1} (black) and fish $\text{h}^{-1} \text{m}^{-1}$ (red) overlaid (C).



DISCUSSION

Two concerns often associated with hydroacoustic methods are known to be (1) unintended noise interferences occurring within the acoustic beam that degrades the signal to noise ratio and impedes fish signal identification (Simmonds and McLennan, 2005; Mitson and Knudsen, 2003; Banneheka *et al.*, 1995), and (2) validation that the fish counts extracted from the raw data are in fact an accurate representation of the fish population sampled (Scouling *et al.*, 2015; Osborne and Melegari 2002; Hartman *et al.*, 2000). The methods presented in this paper are intended to address both of those concerns. We presented an approach to minimize noise interferences at varying range and intensity to maximize fish detection probabilities and create a standardized fish

abundance index, which is comparable across temporal dimensions. We also offered a validation process to quantify the accuracy of automated fish counts by comparing the margins of error among the percentile used for noise removal and masking procedures, and fish tracking parameters used in the automated count process.

Implementing the noise masking procedure allowed us to utilize the maximum range sampled by the acoustic beam without having to create range-specific algorithms for every tidal height and spurious noise signature present. It is important to note that a large beam-masked-percentage did not directly result in lower fish counts. The beam-masked-percentages merely reflect the amount of noise present in the dataset that was masked to identify fish signals more accurately. For high tide, for example, it was necessary for a higher percentage of the beam to be masked than at low tide (Figure 1.7) for the accuracy of automated fish signal identification to remain acceptable (Figure 1.8) as noise levels increased during high tide. If the masked areas remained unmasked, the algorithm would count many of these high noise regions at high tide as fish targets, causing overestimation of fish numbers present. This became evident in the *resample percentile* analysis used to determine the most accurate percentile value used for the noise masking procedure. As the *resample percentile* parameter was the most decisive variable in classifying noise contaminated regions, the value used for this parameter determined how much noise was masked from the dataset. When the algorithm was run at low percentiles, much of the noise within the data remained, resulting in an overestimate of fish present. When the algorithm was run at high *percentiles* (80-90), the algorithm masked out fish data as well as the noise, causing an underestimation of fish present. The optimal *percentile* used in the masking procedure would therefore be able to mask out

noise interferences while maintaining fish targets. The optimal *percentile* used in the masking procedure was determined to be 70, as it displayed the smallest margin of error when comparing automated fish counts to manual fish counts (Figure 1.9).

An alternate approach to masking regions with poor signal to noise ratios (SNR) in the midfield of the beam would be to disregard those high noise regions by simply placing a constant maximum range line at a fixed range, after which the SNR begins to decrease for all files. However, this would result in sampling only a small fraction of the river profile and neglect any fish present in the far field region of the beam. In our dataset, if only the first 15 m of the entire dataset were processed, a range at which the SNR was acceptable for all times sampled, the data used would only reflect 40% of the range data available when applying the methods described in this paper. In other words, this approach enabled us to recover 60% of the data that otherwise would have been lost due to noise. Using only nearfield data would retain sporadic noise sources in the nearfield beam which occur during boat passage, for example. Clearly, data reduction to the nearfield, with the best SNR, would not present a reliable fish abundance estimate.

Fish abundance standardized by sampling range allows for temporal comparisons of fish counts detected with different maximum sampling ranges. Variability in the sampling range over time ultimately creates a bias when comparing fish abundance numbers across temporal dimensions, as the probability of fish detection increases with each additional meter sampled. This is similar to the CPUE concept, where the number of fish caught must be standardized by the effort put forth to achieving that catch, whether it be fishing time, number of vessels, number of tows, or area fished (Kendrick and Bentley, 2010). In our case, the bias was removed by standardizing the fish abundance

numbers by the range sampled. To compare fish abundances across temporal dimensions, where a difference of up to 45 m was recorded in the range sampled between high and low tides of the river (Figure 1.6), the standardized metric of fish $\text{h}^{-1} \text{m}^{-1}$ was used. When applying this standardization method, we observed that numerous fish abundance peaks were muted because there was simply a larger sampling range during those periods (Figure 1.12C).

We chose to standardize by meters sampled rather than volume sampled, due to the difficulty of assessing all factors involved in calculating an accurate beam volume at any given time sampled (Steig *et al.*, 2010). To gain an accurate estimate of the volume sampled by the acoustic beam one would have to incorporate the following variables: (1) the volume of water per unit time varies with the flow rate of the river, (2) any objects detected in the nearfield beam limit the possibility for fish detection in the far field beam for the duration that they remain in the beam, and (3) the inconsistency of the geometric shape of the acoustic beam due to part of the beam encountering the changing river surface. With the objective to obtain a general fish abundance estimate over long-term monitoring, we applied a simpler spatial standardization unit of meters sampled, rather than volume sampled.

A critical component of hydroacoustic data analysis is the inclusion of a validation technique that describes the margins of error expected based on the assumptions made for the data analysis procedure (Hartman *et al.*, 1999, Frear 2002). Hydroacoustics uses sound backscatter as a proxy for fish numbers (Simmonds and McLennan, 2005). As with any proxy used in scientific measurements, hydroacoustics is not a perfectly accurate method to measure fish numbers present. Validation techniques

for hydroacoustic data processing used in previous studies involved manual tracking (Osborne and Melegari 2002), electrofishing (Hughes and Hightower 2015), gill netting (Hughes and Hightower 2015, Baldwin and McLellan 2008), and comparing single, dual and multi beam assemblages (Maxwell and Gove 2007). The known dataset used for our algorithm's validation procedure was derived from visual counts of fish backscatter on the raw TS echogram file. Visual counts of fish backscatter were not a perfect measurement of how many fish were present in the file. Some fish patterns in the raw TS echogram are ambiguous and might be deemed to be a fish by some observers, but not by others. We attempted to be consistent with the quality of manual counts but expect that some variation among researchers remains. The validation method offered in this paper merely assumes a known dataset of fish targets to ground truth the noise removal and fish tracking algorithm. Methods for achieving a known dataset are at the liberty of the researcher, e.g., counting fish in a set period. Once this is established the algorithm validation process described in this paper could be used to quantify the accuracy of the algorithm for the known dataset.

The fish abundance time series developed here gives an estimate of fish numbers present at a study site over time, which can be analysed to learn more about the biological processes in this tidal river. The increase in fish abundance from October to December is most likely the result of diadromous fish migration patterns in the Penobscot River during this time (Saunders *et al.*, 2006). Juvenile alewives in particular have been observed to migrate in the Penobscot River during this time of year and are likely responsible for the pronounced increase in fish counts observed.

The use of hydroacoustic techniques in fisheries research is a growing field (Trenkel *et al.*, 2011). Benefits associated with the extensive spatial component applicable over broad temporal scales make this technology an attractive method for studies involving fish abundance estimates and population studies to assess management guidelines (Daum *et al.*, 2006). Applying a standardization method to compare datasets of different temporal and spatial scales allows for this technique to be used in long term monitoring studies where variable environmental conditions could be reflected in the data. With a well-founded validation method in place to evaluate the accuracy of automated fish counting algorithms, we look to apply the methods-based approach described in this paper to three more six-month datasets associated with the Penobscot River Restoration Project. Ultimately, we intend to compare fish abundance estimates from pre-dam removal years to post-dam removal years, and examine whether changes in fish abundance are observed in this part of the river after dam removal.

REFERENCES, CHAPTER 1

- Baldwin, C. M., and J. G. McLellan. 2008. Use of gill nets for target verification of a hydroacoustic fisheries survey and comparison with kokanee spawner escapement estimates from a tributary trap. *North American Journal of Fisheries Management*, 28: 1744-1757.
- Ballón, M., Bertranda, A., Lebourges-Dhaussyc, A., Gutiérrezd, M., Ayóna, P., Gerlottob, D.G.F. 2011. *Progress in Oceanography*, 91: 360-381.

- Banneheka, S.G., Routledge, R.D., Guthrie, I.C., Woodey, J.C. 1995. Estimation of in-river fish passage using a combination of transect and stationary hydroacoustic sampling. *Canadian Journal of Fisheries and Aquatic Sciences*, 52: 335-343.
- Bentley, N., Kendrick, T.H., Starr, P.J., Breen, P.A. 2011 Influence plots and metrics: tools for better understanding fisheries catch-per-unit-effort standardizations. *ICES Journal of Marine Science*, 69: 84-88.
- Daum, D.W., Osborne, B.M. 1998. Use of fixed-location, split-beam sonar to describe temporal and spatial patterns of adult fall chum salmon migration in the Chandalar River, Alaska. *North American Journal of Fisheries Management*, 18: 477-486.
- De Robertis, A.D., Higginbottom, I. 2007. A post-processing technique to estimate the signal- to-noise ratio and remove echosounder background noise. *ICES Journal of Marine Science*, 64: 1282- 1291.
- Echoview Manual Pty Ltd (2015). Echoview software, version 6.1.44. Echoview Software Pty Ltd, Hobart, Australia.
- Fraser, S., Nikora, V., Williamson, B.J., Scott, B.E. 2017. Automatic active acoustic target detection in turbulent aquatic environments. *Limnology and Oceanography: Methods*, 00: 00-00.
- Frear, P.A. 2002. Hydroacoustic target strength validation using angling creel census data. *Fisheries Management and Ecology*, 9: 343-350.

- Hartman, K.J., Nagy, B., Tipton, R.C., Morrison, S. 2000. Verification of hydroacoustic estimates of fish abundance in Ohio River lock chambers. *North American Journal of Fisheries Management*, 20: 1049-1056.
- Hughes, J.B., Hightower, J.E. Combining split- beam and dual- frequency identification sonars to estimate abundance of anadromous fish in the Roanoke River, North Carolina. *North American Journal of Fisheries Management*, 35: 229-240.
- Kendrick T. H., Bentley N. 2010. Fishery characterization and catch-per-unit-effort indices for trevally in TRE 7, 1989-90 to 2007-08. *New Zealand Fisheries Assessment Report*, 2010/41pg. 58 pp.
- Kieser, R., Reynisson, P., and Mulligan, T. J. 2005. Definition of signal-to-noise ratio and its critical role in split-beam measurements. *ICES Journal of Marine Science*, 62: 123–130.
- Klevjer, T.A., Kaartvedt, S. 2003. Split-beam target tracking can be used to study the swimming behavior of deep-living plankton in situ. *Aquatic Living Resources*, 16: 293 -298.
- Koslow, A.J. 2009. The role of acoustics in ecosystem- based fishery management. *ICES Journal of Marine Science*, 66: 966-973.
- Krumme, U. 2004. Patterns in tidal migration of fish in a Brazilian mangrove channel as revealed by a split-beam echosounder. *Fisheries Research*, 70: 1-15.
- Love, R.H. 1977. Target strength of an individual fish at any aspect. *Journal of the Acoustical Society of America*, 62: 1397-1403.

- Mann, D. A., Hawkins, A. D., & Jech, J. M. (2008). Active and passive acoustics to locate and study fish. In *Fish bioacoustics* (pp. 279-309). Springer New York.
- Maxwell, S.L., Gove, N.E. 2008. Assessing a dual-frequency identification sonar's fish-counting accuracy, precision, and turbid river range capability. *The Journal of the Acoustical Society of America*, 122: 3364-3377.
- Misund, O.A., Beltestad, A.K. 1996. Target-strength estimates of schooling herring and mackerel using the comparison method. *ICES Journal of Marine Science*, 53: 281-284.
- Mitson, R. B., and Knudsen, H. P. 2003. Causes and effects of underwater noise on fish-abundance estimation. *Aquatic Living Resources*, 16: 255-263.
- Osborne, B.M., Melegari, J.L. 2002. Use of split-beam sonar to enumerate Chandalar River fall chum salmon, 2000. *Alaska Fisheries Technical Report Number 61*.
- Rudstam, L.G., Schaner, T., Gal, G. Boscarino, B.T., O'Gorman, R., Warner, D.M., Johannsson, O.E., Bowen, K.L. 2008. Hydroacoustic measures of *Mysis relicta* abundance and distribution in Lake Ontario. *Aquatic Ecosystem Health & Management*, 11: 355-367.
- Samedy, V., Wach, M., Lobry, J., Selleslagh, J., Pierre, M., Josse, E., Boët, P. 2015. Hydroacoustics as a relevant tool to monitor fish dynamics in large estuaries. *Fisheries Research*, 172: 225-233.
- Saunders, R. Hachey, M.A., Fay, C.W. 2006. Maine's diadromous fish community: past, present, and implications for Atlantic salmon recovery. *Fisheries* 31: 537-547.

- Scouling, B., Chu, D., Ona, E., Fernandes, P.G. 2015. Target strengths of two abundant mesopelagic fish species. *Journal of the Acoustical Society of America*, 137: 989-1000.
- Similä, T. 1997. Sonar observations of killer whales (*Orcinus orca*) feeding on herring schools. *Aquatic Mammals*, 23: 119-126.
- Simmonds, J., MacLennan, D. 2005. Biological Acoustics. In *Fisheries Acoustics Theory and Practice*, 2nd edn, pp. 158-162. Blackwell Science, Oxford, UK.
- Steig, T.W., Nealson, P.A., Sullivan, C.M., Ehrenberg, J.E. 2010. Development of a method for estimating the probability of detecting fish through a hydroacoustic beam. *Oceans 2010 MTS/IEEE Seattle*, Seattle, WA: 1-13.
- Swartzman, G., Silverman, E., Williamson, N. 1995. Relating trends in walleye pollock (*Theragra chalcogramma*) abundance in the Bering Sea to environmental factors. *Canadian Journal of Fisheries and Aquatic Sciences*, 52: 369-380.
- Trenkel V.M., Ressler, R.H., Jech, M., Giannoulaki, M., Tayler, C. 2001. Underwater acoustics for ecosystem-based management: state of the science and proposals for ecosystem indicators. *Marine Ecology Progress Series*, 442: 285-301.
- Viehman, H.A., Zydlewski, G.B., McCleave, J.D., Staines, G.J. 2015. Using hydroacoustics to understand fish presence and vertical distribution in a tidally dynamic region targeted for energy extraction. *Estuaries and Coasts*, 38: 215-226.
- Zhang, J., Zuo-zhi, C., Guo-bao, C., Peng, Z., Yong-song, Q., Zhuang, Y. 2015. Hydroacoustic studies on the commercially important squid *Sthenoteuthis oualaniensis* in the South China Sea. *Fisheries Research*, 169: 45-51.

CHAPTER 2:
USING HYDROACOUSTICS TO RELATE FLUCTUATIONS IN FISH
ABUNDANCE TO RIVER RESTORATION EFFORTS
AND ENVIRONMENTAL CONDITIONS IN
THE PENOBSCOT RIVER, MAINE

ABSTRACT

Quantifying how fish abundance changes after a significant portion of their natural habitat becomes re-accessible is critical to gauge the success of large restoration efforts. Because fish abundance also changes with naturally fluctuating environmental conditions, examining abundance relative to these conditions can indicate fish responses to both anthropogenic and natural river variation. A side-looking hydroacoustic system was used to estimate fish abundance in the Penobscot River, ME from 2010-2016, where 2010-2013 were pre-dam removal conditions, and 2014-2016 were post-dam removal conditions. The river was monitored during non-ice condition periods, roughly May to November annually. Automated data processing enabled continuous abundance estimates from fish tracks. A fourfold increase in median fish abundance occurred in the fall compared to spring and summer, regardless of dam presence. Concurrent with restoration activities, fish abundance increased approximately twofold pre- to post-dam removal. We examined the influence of natural environmental conditions including tide, discharge, temperature, diurnal cycle, day length, moon phase, as well as restoration activities (focusing on dam presence) on variability in fish abundance. Daylength (or photoperiod) was the most important predictor variable in all eight time-series analyzed. During the

fall migration, abundance was generally higher during outgoing tides, at night, and during relatively high river discharge. In the early fall, when daylength was between 11.28 h and 12 h (September 24th to October 6th) and water temperature was above 11.96 °C, an eightfold increase in fish abundance was recorded in post-dam removal years. Alewife stocking numbers increased post-dam removal relative to pre-dam removal years and likely contributed to the increased fish abundance detected. This is one of the first validated tools to continuously examine the response of fish abundance to a major river restoration activity. In this application, it significantly increased our understanding of how fish abundance changed in the Penobscot River as result of major restoration efforts and provides a basic understanding of fish responses to naturally fluctuating environmental conditions.

INTRODUCTION

Diadromous fish play an important role in improving and sustaining healthy riverine, estuarine, and marine ecosystems, yet their populations are in serious decline (Saunders et al. 2006). Ecosystems depend on these species collectively for: (1) the delivery of marine derived nutrients (Durbin et al. 1979; Kline et al. 1990); (2) prey for other fish species (Schulze 1996), marine mammals (Cairns and Reddin 2000), birds (Wood 1986), and terrestrial vertebrates (Cederholm et al. 1989); and (3) reducing the probability of predation for less abundant fish species (Saunders et al. 2006). The decline of diadromous fishes in the northeastern United States has largely been attributed to human influences including the damming of rivers, overfishing, and pollution (Moring

2005). Recent regulatory and environmental conservation efforts have limited the negative effects of overfishing via the Magnuson Stevens Act, while a combination of industrial decline and stricter environmental policies, such as the Clean Water Act, have decreased pollutants dramatically.

Today, perhaps the biggest challenge for diadromous fish species is damming of river systems for hydroelectric power generation or flood control (NRC 2004; Gephard 2008). In 2004, the Penobscot River Restoration Project (PRRP) was implemented by the Penobscot River Restoration Trust (PRRT). A key element of this restoration project was the removal of Great Works Dam in 2012 and Veazie Dam in 2013. Veazie Dam was located just upstream of the head of tide, while Great Works Dam was located 13 km upstream from Veazie Dam. These dam removals opened 14 km of additional river habitat for diadromous fish. In 2014, a fish lift was installed at Milford Dam to improve fish passage at the now lowermost dam located 14 river km upstream from the removed Veazie Dam. To jump-start fish abundance increases, stocking efforts were increased for alewife (*Alosa pseudoharengus*) beginning in 2010 and increasing through 2016. If successful, the project was designed to not only revive the native fisheries of the region, but also bring economic, social and cultural benefits to the communities of the Penobscot region (Opperman et al. 2011). Economic, ecological, and socio-economic values of fisheries generally increase following ecosystem restoration efforts, as higher species richness leads to more complex ecosystems, lower volatility, and higher value trophic levels of fish species (Sumaila et al. 2000). However, specific case studies showing a quantitative account of restoration efforts in terms of fish abundance changes are lacking. The Penobscot River Restoration Project was a great opportunity to provide an indication

of what may be expected from river restoration efforts including dam removal. Quantifying the success of such a large restoration effort would not only provide a valuable indicator for fish abundance recovery due to dam removal, but also give other communities a model to draw on for decision-making (Trinko-Lake et al. 2012).

The goal of the PRRP was to restore 11 species of sea-run fish to the Penobscot River, while maintaining energy production. Specifically, this project aimed to increase the abundance of all 11 native diadromous fish species. With over 14 km of additional river habitat directly available after dam removal, nearly half of the native species (Atlantic sturgeon, *Acipenser oxyrinchus oxyrinchus*; Atlantic tomcod, *Microgadus tomcod*; rainbow smelt, *Osmerus mordax*; endangered shortnose sturgeon, *Acipenser brevirostrum*; and striped bass, *Micropterus salmoides*) had 95-100% of their historic habitat restored (Trinko-Lake et al. 2012; Saunders et al. 2006). Alewife, blueback herring (*Alosa aestivalis*), American shad (*Alosa sapidissima*), American eel (*Anguilla rostrata*), sea lamprey (*Petromyzon marinus*), and endangered Atlantic salmon (*Salmo salar*) now have access to as much as two-thirds of their historic habitat (Opperman et al. 2011). With a great percentage of their historic habitat available again, it is crucial to monitor the relative change in abundance of these species in the lower reach of the Penobscot River.

Fish abundance and species assemblages vary seasonally in rivers with large diadromous fish populations (Iafate et al. 2008). Both downstream and upstream migration timing and intensity in rivers are influenced by water flow, water temperature and photoperiod (daylength; Jonsson 1991). For example, photoperiod and temperature, have been identified as triggers for initiating downstream migratory behavior of Atlantic

salmon smolts (Martin et al. 2012). Large seasonal differences in fish abundance and species composition were documented in upper San Francisco estuary are largely controlled by fluctuations in salinity and temperature, with the lowest abundance occurring in winter and spring, and the highest abundance in summer and fall (Gewant and Bollens 2012). Gewant and Bollens (2012) developed a fish count metric that normalized the catch rate of fish by sampling site and effort. However, establishing such standardized measures of abundance over long time series is challenging and not common-place.

Most traditional approaches to document variation in fish abundance are spatially and temporally limited (e.g. fyke nets; Gewant and Bollens 2012) and focus on individual fish rather than total abundance. Tagging techniques, trawling, and electrofishing are all sampling techniques that yield sporadic fish abundance and species estimates, providing good spatial coverage (Kiraly et al. 2015; Watson 2017), but poor temporal resolution. To investigate changes in total fish abundance in a river and how it varies in response to different river and environmental conditions, a continuous sampling technique for fish abundance would be optimal to yield high temporal resolution time series of relative fish numbers in a single location. Hydroacoustic monitoring techniques are often used to meet such requirements (Rudstam et al. 2012; Trenkel et al. 2011).

Hydroacoustic technologies have been used by fisheries researchers to count the number of diadromous fish passing through a given area continuously (millisecond resolution) over time, providing an indicator of fish presence. For example, down-looking, mobile hydroacoustic techniques have been applied to estimate the number of adult spawners returning to the Roanoke River, North Carolina, USA, and identify

seasonal pulses of hickory shad (*Alsos mediocris*), American shad, and striped bass (Mitchell 2006). Fixed-location, bottom-mounted, upward-looking hydroacoustic transducers were deployed in the Baltic Sea to study diel patterns in pelagic fish behavior, including Baltic herring (*Clupea harengus*), sprat (*Sprattus sprattus*), and smelt (*Osmerus eperlanus*) (Axenrot et al. 2004). Fixed-location, side-looking (horizontally oriented) hydroacoustic methods have been used to estimate the abundance of migrating Chinook salmon (*Oncorhynchus tshawytscha*) in the Kenai River, Alaska (Burwen et al. 2003).

Fish abundances in the Penobscot River are known to vary seasonally due to the suite of species assemblages and variation in the population sizes present (Saunders et al. 2006). Adult anadromous fish species, such as alewives, blueback herring, and American shad immigrate to freshwater rivers to spawn in the late spring to early summer, while their young begin their emigration to the ocean in the fall (Mullen et al. 1986). Other anadromous fish species, such as adult Atlantic salmon immigrate in the spring and throughout the summer to headwater streams to spawn. Their offspring will use tributaries as foraging grounds for one to two years before emigrating to the ocean to continue their life cycle (Zydlewski and Zydlewski 2012). The American eel, a catadromous species, is known to immigrate as juveniles in the spring to early summer, mature in tributaries for years to decades and finally emigrate as adults to the ocean in the fall. As such, migratory behaviors vary within the Penobscot River, giving the river a dynamic flux of fish throughout the year.

We aim to gain a better understanding of how the migratory periods of diadromous fishes vary within a migratory year as well as among years, and how that

variation may be explained by environmental conditions, including restoration efforts. Results derived from this study provide an indication of the changes a river undergoes after restoration efforts, and indicate what environmental conditions influence fish abundance variability in the Penobscot River. The goals of this study were to investigate: 1) changes in total fish abundances pre- and post-dam removal, 2) seasonal variability in fish abundances in both pre- and post-dam removal years, and 3) how fish abundance variability was related to different river and environmental conditions, including the increased stocking efforts associated with the river restoration. Finally, we qualitatively compared changes in fish abundance to other, parallel studies of fish presence in the Penobscot River to explore the utility of this method as an indicator of how fish abundances respond to dam removal.

METHODS

Sampling procedure

BioSonics side-looking split-beam hydroacoustic technology was used to estimate fish abundances (defined as fish $\text{h}^{-1} \text{m}^{-1}$) in the Penobscot River, ME. Transducers were deployed on both sides of the river (Table 2.1); projecting an acoustic beam across the river from each side (Figure 2.1). Looking upstream, the station on the left river bank was designated Pen A, while Pen B was located on the right river bank (Figure 2.1). The study site was 5 km downstream of the Veazie Dam removed from the river in 2013 (Figure 2.2). Average tidal ranges at the study site span 5.25 m. Surveys began in 2010 and continued through 2016. Data collection was only possible from May to

approximately November of each year since the Penobscot River was subject to icy conditions that could compromise equipment between the months of November to April. Ice was likely to cause unwanted interference signals in the acoustic transducer beam and posed a collision threat to the equipment. The exact deployment dates varied each year due to variation in the ice-out date for the river (Table 2.1).

Figure 2.1. Cross-sectional illustration of the experimental setup at the survey sites in the Penobscot River. Bottom topography was mapped by conducting down-looking hydroacoustic transects across the river (green lines in main image, red lines in inset). The bottom right inset shows the cross-river transects in an overhead Google Earth view.

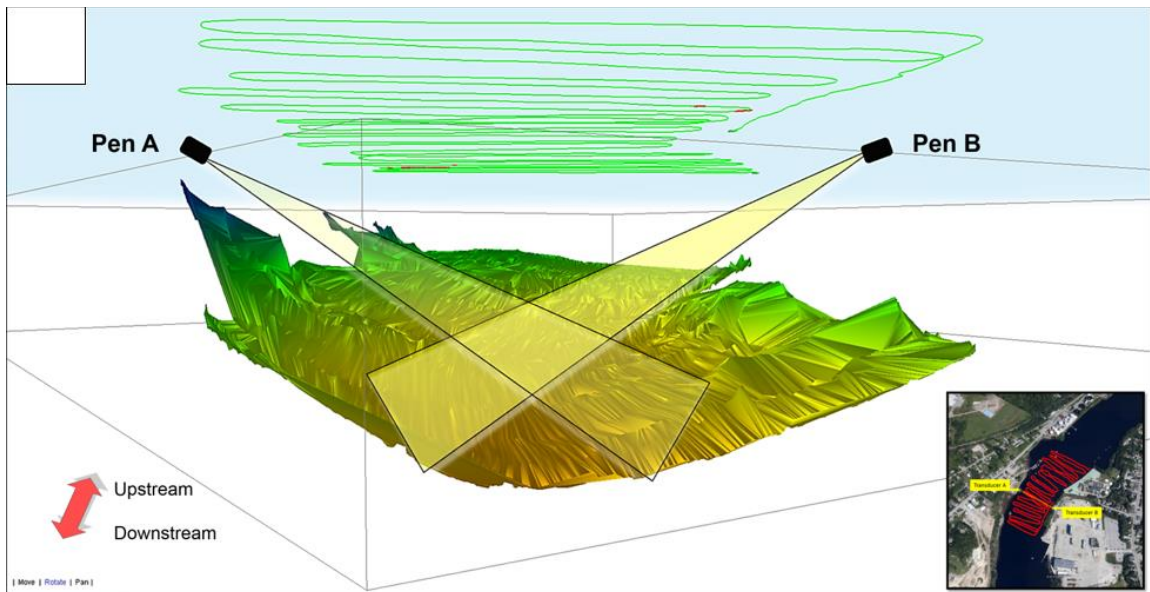
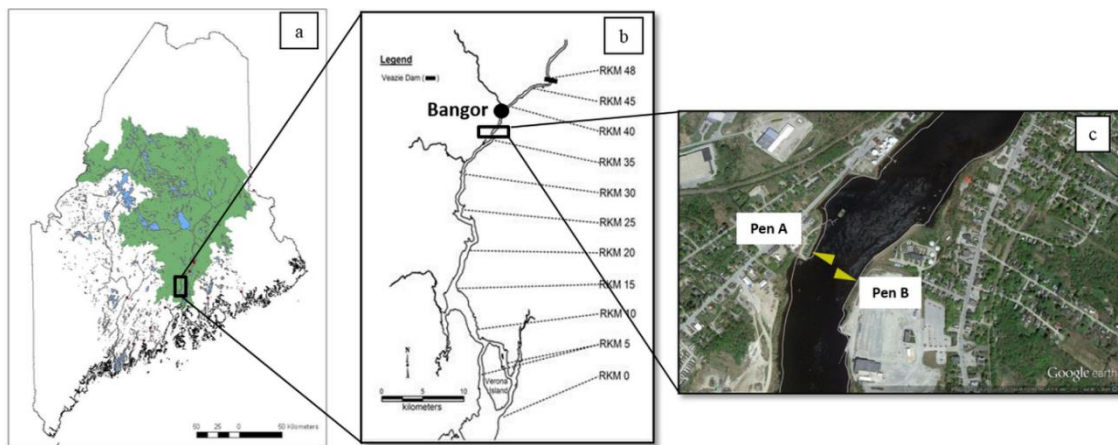


Table 2.1. Annual dates for side-looking deployment of BioSonics split beam transducers in the Penobscot River, Maine. Pen A and Pen B are the respective split beam transducers and associated transceiver systems deployed on the Western and Eastern sides of the River, respectively.

Year	Pen A				Pen B			
	Transducer Type	Beam angle (Major, Minor)	Deployed	Removed	Transducer Type	Beam angle (Major, Minor)	Deployed	Removed
2010	430 kHz	6.8°, 6.8°	Aug. 27	Nov. 4	206 kHz	6.8°, 6.8°	Apr. 27	Nov. 18
2011	208 kHz	3.6°, 10.4°	May 18	Oct. 26	208 kHz	3.6°, 10.5°	Apr. 29	Dec. 9
2012	208 kHz	3.6°, 10.4°	May 28	Oct. 26	208 kHz	3.6°, 10.5°	Apr. 18	Nov. 20
2013	208 kHz	3.6°, 10.4°	May 15	Nov. 11	208 kHz	3.6°, 10.5°	May 1	Oct. 25
2014	Transition year – No comparable data collected							
2015	206 kHz	6.6°, 6.6°	May 20	Dec. 7	206 kHz	6.5°, 6.5°	May 7	Nov. 17
2016	206 kHz	6.6°, 6.6°	May 7	Nov. 13	206 kHz	6.5°, 6.5°	Apr. 26	Nov. 8

Figure 2.2. Map of Penobscot watershed in Maine and relative location of the study site. Map produced by Zydlewski and Staines in prep. a) the Penobscot watershed is shaded in green; b) River sections marked by river km starting at the mouth of the river entering Penobscot Bay and ending at the previous Veazie Dam location at rkm 48; c) satellite image of the river section sampled using hydroacoustics, the yellow triangles represent the approximate coverage of the two beams.



Data quality assessment

Early deployment years were often subject to technical difficulties that limited the functionality of the transducers. These difficulties, caused by poor transducer aim and physical beam restrictions as a function of large side-lobes and unwanted transducer cross-talk, resulted in some sampling periods being unsuitable for fish abundance estimates (Table 2.2). In addition, changing of the transducer beam angle and collection frequency by switching transducers within a sampling year caused some periods of data to be either unsuitable for processing, or were not comparable to the remaining years.

Sampling periods with severely compromised data quality and range (2010 Pen B, 2012

Pen A, 2013 Pen A & B) were not used. Data suitability was determined using a data quality evaluation procedure for each deployment period. Data quality was assessed for a subsample of 90, 15-minute files that were randomly selected for each collection year and river side. Each file was evaluated to assess whether good data quality could be generated for at least the first 15 m from the transducer. Data quality was considered “good” when fish counts could be extracted.

Table 2.2. Relative data quality of archived side-looking hydroacoustics data collected in the Penobscot River, ME. Sampling years and river sides were deemed appropriate for automated processing based on the data quality present in a subsample of 90, 15-minute files. Green blocks indicate algorithms that were constructed for this dataset, while red blocks indicate that no accurate fish track information could be extracted.

State	Year	Pen A (West Shore)	Pen B (East Shore)
Pre-dam Removal	2010	Red	Red
	2011	Green	Green
	2012	Red	Green
	2013	Red	Red
Post-dam Removal	2014: <i>transition year</i>	No comparable data collected	
	2015	Green	Green
	2016	Green	Green

The range (distance from the transducer) of good data quality was specified as the range at which fish and noise could be distinguished using the automated processing approach described in Chapter 1. Briefly, this involved determining the maximum range at which the acoustic noise within a spatiotemporal region of 2 m by 300 pings (2 m by 75 seconds at 4 pings per second) exceeded the acoustic threshold of -49 dB. With the fish target threshold set at -45 dB, -49 dB represented a noise level where fish targets were no longer clearly distinguishable from the acoustic noise within each cell. This process provided a distinct interface between regions where fish were detectable and undetectable due to background noise, that could be determined using automated data processing. The maximum range line was indicative of the range at which the transducer's acoustic beam encountered a strong interference object (*i.e.*, river bottom or surface). For all files, if a maximum range line could not be drawn using the automated process described, the data being collected was deemed not viable for automated fish detection. In this case, even the river bottom (or surface) did not elicit a strong enough signal to be measured, and deciphering a fish signal would be highly unlikely. Therefore, if the number of files with inappropriate sampling ranges for the data subsample was above 10% for that year, we omitted that year and/or river side for data processing. When the number of files was within 10% of the number of files subsampled we constructed a processing algorithm for that year and river side. Based on this evaluation, part of 2010 (after a 430 kHz transducer was installed in August), 2011, 2015, and 2016 were selected from the Pen A side for data processing, and 2011, 2012, 2015, and 2016 were selected from the Pen B side (Table 2.2).

Automated data processing

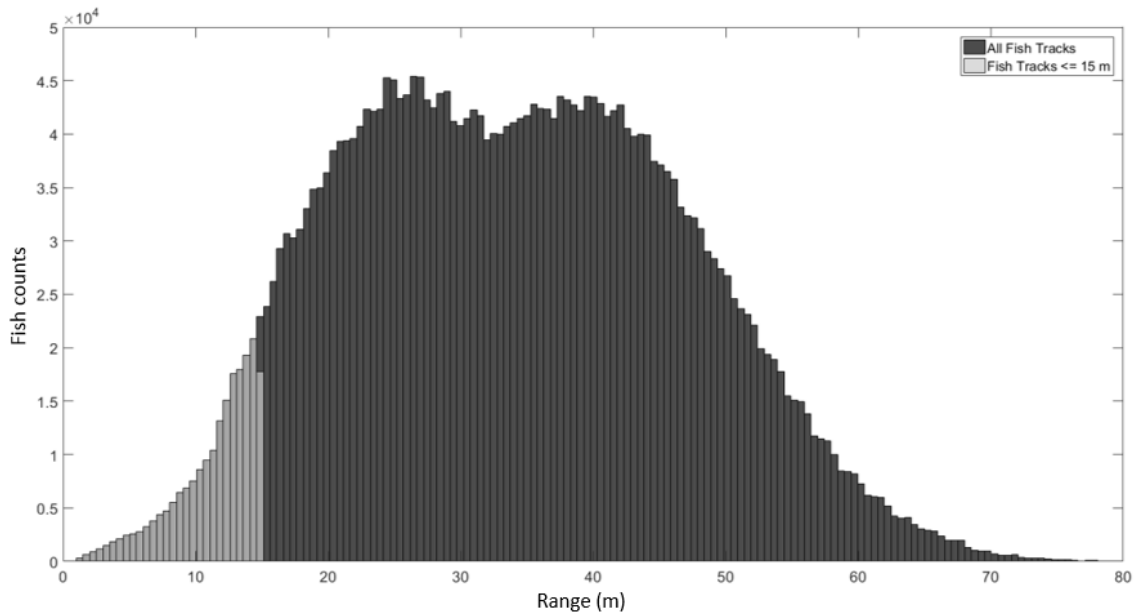
A standardized processing approach (Chapter 1) was used to generate and apply year and river-side specific hydroacoustic processing algorithms in Echoview. Briefly, this approach involves a cell-based noise removal approach where midfield beam interferences potentially causing false fish signal classifications were masked, and a maximum range line was drawn at the range from the transducer where fish targets were indistinguishable from background noise (see data quality assessment). Tidal fluctuations caused variability in midfield beam interferences and maximum range detection, as the volume sampled by the acoustic beam would change according to the river depth based on the tides. Noise levels within each cell would change over time based on the varying noise signatures caused by the tides. Based on the spatiotemporal metric of each cell (2 m by 300 pings), the maximum range line and mask applied to remove midfield beam interference could adjust by the metric of one cell at its minimum, when the noise level threshold of -49 dB was exceeded. Once the maximum range line was identified, and midfield beam interferences masked, the potential fish targets remaining were determined to be fish tracks based on the spatiotemporal proximity of potential fish targets to others detected in the beam. Each fish track was characterized as one fish count. Information recorded for each fish track included depth, velocity, target strength (TS), directionality, and range from transducer. Fish counts were binned by hour (number of tracks per hour) and divided by the median range sampled for each hour to produce spatiotemporally standardized fish abundance estimates (fish h⁻¹ m⁻¹). Once applied, the exported fish abundance data was used to construct a continuous time series of fish abundance estimates for each year and river side. Each year's algorithm was validated through an

independent subsample of data files on which manual fish counts were made and correlated with the automated fish counts derived from each year and river sides' automated processing algorithm. Final algorithms used had a regression coefficient of at least 0.85 and were applied to the entire hydroacoustic dataset of each year and river side.

Data correction for range

Using a range standardization method to create a temporally comparable metric assumes detection probability remains constant with each additional meter sampled. However, the number of fish counts increased with increasing range sampled, with the greatest number of counts being observed between 25 m and 40 m ranges (Figure 2.3). A bimodal distribution can be observed when examining fish counts by range due to the sampling range extending to 25 m and 40 m more frequently. Fish located at 25 m and 40 m ranges were sampled more frequently, thus causing total fish counts in these ranges to be higher. When examining variability in fish abundances inter-annually and between pre- and post-dam removal years, it was important to use a standardized fish abundance metric where fish detection probabilities were as similar as possible for all years sampled.

Figure 2.3. Histogram of all fish tracks detected by range. $N = 3,298,789$. The light-grey area depicts all fish counts within 15 m of the transducer, which represents 6.34% of all fish tracks detected ($N = 209,143$) and was used to estimate changes in fish counts pre- and post-dam removal (Figure 2.7). The combined dark-grey and light-grey areas were used to assess changes in seasonal fish abundance and for CART analysis. All fish counts, after being binned by sampling hour, are represented in the fish abundance time series plot (Figure 2.5) and seasonal fish abundance plots (Figure 2.8) as part of the range standardized fish count metric $\text{fish h}^{-1} \text{m}^{-1}$.



Since median sampling ranges varied significantly between each year and river side, we decided to compensate for the remaining range bias by also only considering fish counts detected within the first 15 m of the acoustic beam when comparing fish counts pre- and post-dam removal. This essentially eliminated range-bias, as nearly 100% of all hours sampled (99%) had a median sampling range above this value. It also mitigated the

effect that the beam angle difference of the transducer types used might have had on fish signal detections, as the volume sampled by the different transducer types only varied by a maximum of 0.45 m³ for the first 15 m sampled (min. = 9.71 m³, max. = 10.16 m³). While this method allowed us to be confident that fish detection probabilities were nearly identical for pre- and post-dam removal comparisons, it also restricted our dataset to only 6.34% of all fish counts made.

When examining seasonal variability in fish abundance and its relation to environmental conditions (discharge, temperature, daylength, diel cycle, moon phase, tide phase, dam conditions, and river side), we used all ranges sampled since this provided the best possible estimate of fish abundances. Fish abundance was defined as a spatiotemporally standardized metric (fish h⁻¹ m⁻¹) to include fish counts from all sampling ranges. This metric was then used to assess seasonal changes in fish abundance, construct fish abundance time series for each year and river side processed, and describe their relation to environmental variables.

Data Analysis

Variation in fish abundance among pre-and post-dam removal years and seasons was examined using Analysis of Variance (ANOVA) techniques. However, data were not normally distributed (Kolmogorov-Smirnov, $p < 0.01$). Therefore, a Wilcoxon rank sum test was used to assess whether differences of total fish abundances between pre- and post-dam removal conditions were significant, and Kruskal-Wallis test was used to test whether total fish abundances varied significantly by season (spring, summer, fall). Seasons were classified using the equinox and solstice where: Spring was defined as

deployment until June 21st; Summer was June 21st to September 21st, and Fall from September 21st until system removal.

We explored the relationship between observed fish abundances and river conditions using Classification and Regression Tree (CART) analysis. The target variable evaluated was the range-adjusted fish count metric (fish h⁻¹ m⁻¹). River and environmental parameters included three continuous predictors: river discharge (m³ s⁻¹), temperature (°C), and daylength (h); and five categorical predictors: diurnality (day or night), tide phase (incoming and outgoing), moon phase (new moon, first quarter, full moon, second quarter), dam condition (present or removed), and river side (Pen A or Pen B).

We used environmental data from a variety of monitoring stations and agencies including United States Geological Survey (USGS; West Enfield, station 01034500, Eddington station 01036390), HOBO depth and temperature loggers deployed at the study site, Penobscot Indian Nation temperature loggers deployed near the study site, and the U.S. Navy Astronomical Applications Department. Numeric values were assigned to all predictors for each active sampling hour recorded by the hydroacoustic system (Table 2.3). Each sampling hour had corresponding values for fish abundance and each environmental condition. Since time was not a predictor, data gaps were ignored, as each sampling hour with a missing fish abundance value would also not be assigned an environmental condition, and thus not used in the CART analysis.

Table 2.3. Numeric values representative of different environmental variable conditions assigned to each sampling hour and used in CART analysis.

<i>Variable</i>	<i>Class</i>	<i>Definition (Condition)</i>	<i>Value</i>
Fish abundance	Target	fish h ⁻¹ m ⁻¹	Continuous
Daylength	Predictor	Daylight hours as a fraction of 24	Continuous
Temperature	Predictor	°C	Continuous
Discharge	Predictor	m ³ s ⁻¹	Continuous
Day, night (diel cycle)	Predictor	Night, day, (dawn & dusk hours)	0, 1, (2 & 3)
Tide phase	Predictor	Outgoing, incoming, slack tide	0, 1, 3
Moon phase	Predictor	New moon, first quarter, full moon, second quarter	1, 2, 3, 4
Dam condition	Predictor	Pre-dam removal, post-dam removal	0, 1
River side	Predictor	Pen A, Pen B	1, 2

Fish abundance data were partitioned based on the associated predictive variable that elicited the greatest difference in the values of the target variable, creating two mutually exclusive groups with maximum homogeneity (Breiman et al., 1984). This process was continuously repeated on the mutually exclusive data groups created to produce a decision tree. Each splitter node in a decision tree identified a condition that sorted fish abundance data by either meeting this condition, or not. Data partitioning continued until a terminal node was reached, signifying that no further splitter conditions were identified, or that user-specified limitations for the CART model were reached. Each node displayed a response value that was predicted based on the conditions of that

node. The number of terminal nodes describes the complexity of a tree. Where a complex tree might best describe the underlying relationship between predictor and response variable and create the most accurate fish abundance prediction values based on this relationship, it is often too complex to read and describe relationships. We present the results of both a complex CART version (unpruned), and a simplified version of the CART analysis.

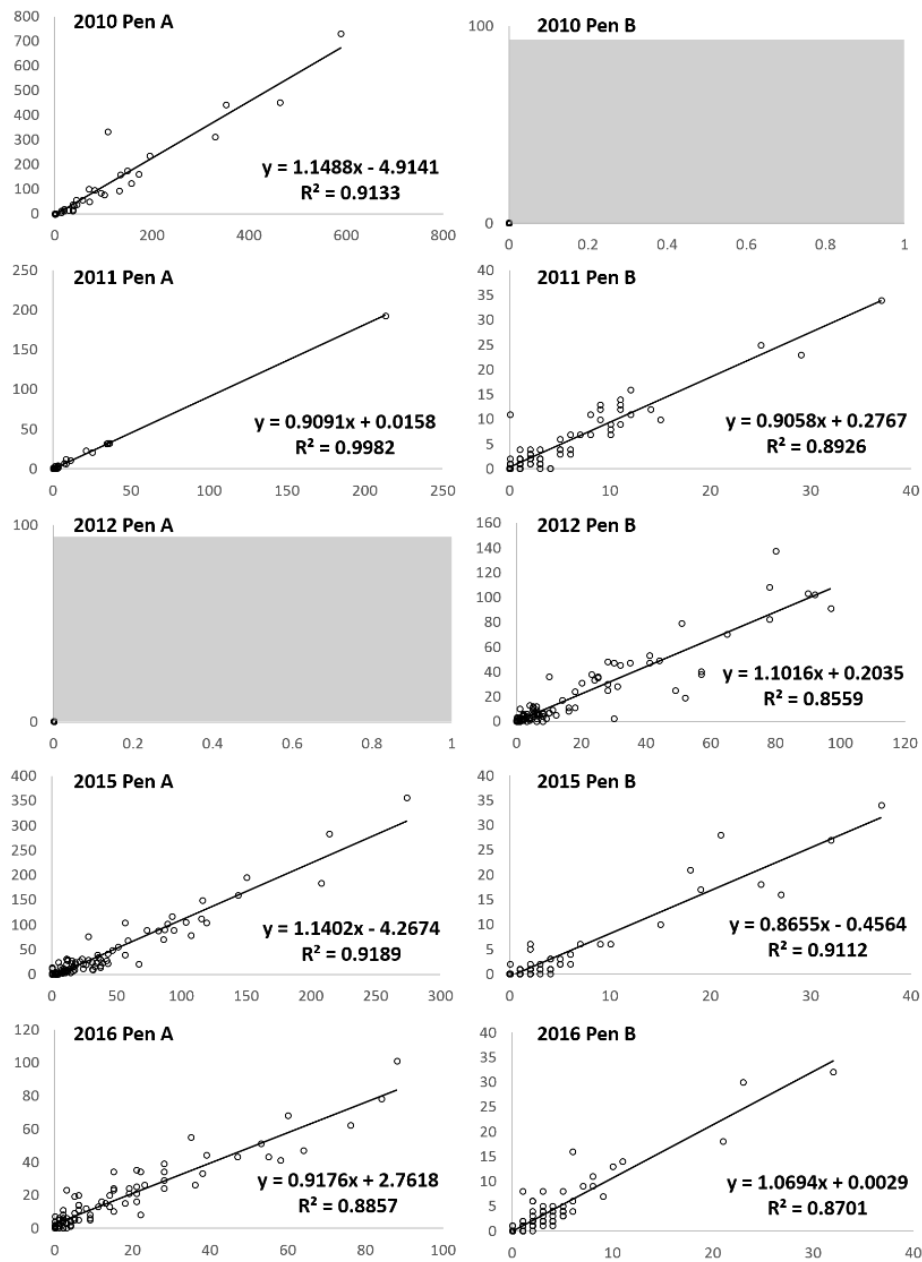
Complex trees of fish abundance split by predictor variables were used to extract the relative importance of those variables, and pruned back to a reasonable size that displayed and described the most important relationships. Terminal node sizes were restricted to contain at least 96 data points (i.e. the condition described in each terminal node must have been present for at least 96 hours or longer). Ninety-six was used as the minimum number of hours needed for a terminal node to be established, as hourly discharge values represented four-day averages, and each specific moon phase was also assigned to the 48 hours before and after its peak occurrence. CART analysis was used to evaluate the relative predictability of each variable, where the most predictive environmental variable assumed a value of 100, and all subsequent predictors assumed a value relative to this predictor. If two predictors were highly correlated, it only used the most significant data splitting variable of the two for establishing the decision tree. CART analyses were conducted through a data processing and data mining program by Salford Systems®.

RESULTS

Automated processing validation

All automated processing algorithms were validated. Automated fish counts per file produced by year and river-side specific algorithms were highly correlated ($R^2 > 0.87$) with manual counts of fish from the same file (Figure 2.4).

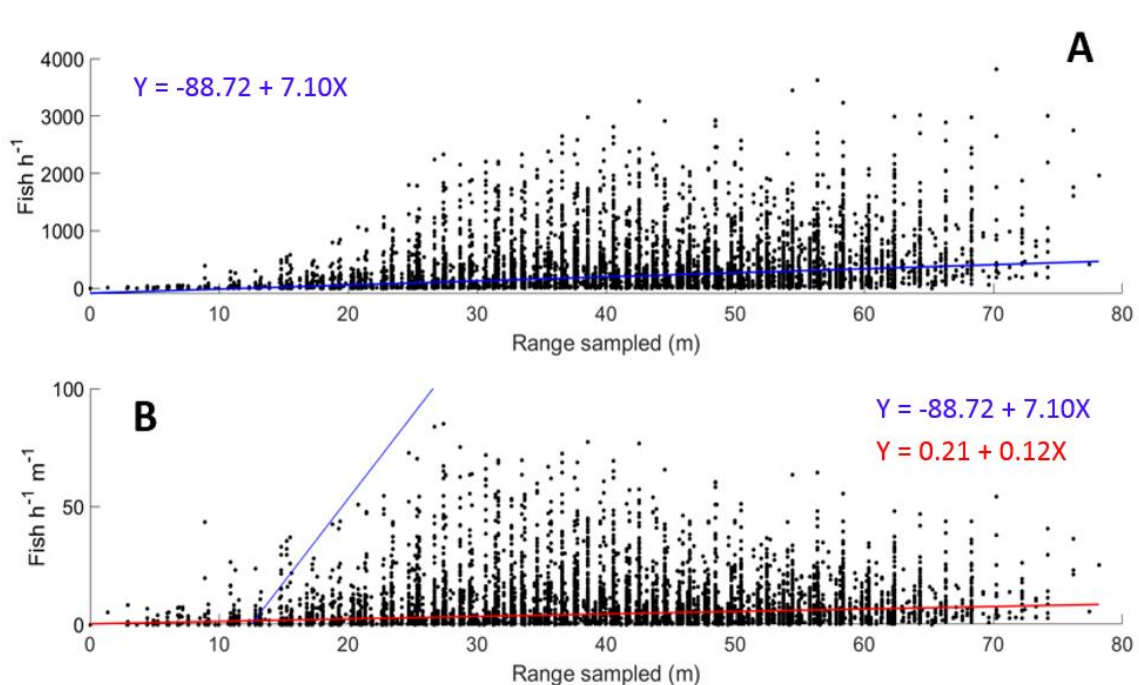
Figure 2.4. Regression plots of automated and manual fish counts for each year and river side sampled in the Penobscot River, ME. The x-axis represents manual counts and the y-axis are automated counts for each file. Regression coefficients (R^2) and slope equations are displayed. Grey boxes signify that data for the specified river side of that year was not of high enough quality for automated processing.



Range standardization

The number of fish counts increased with increasing range. For all ranges sampled, the number of fish h^{-1} increased with range (Figure 2.5A) with a slope of 7.1. When standardized by the median range sampled for each hour, the increase in fish h^{-1} for each additional meter sampled are reduced to a slope of 0.1 (Figure 2.5B). Where fish h^{-1} are largely dependent on the range sampled, the range-standardized fish abundance metric (fish $\text{h}^{-1} \text{m}^{-1}$) was used to compare sampling hours with significantly different sampling ranges, as the fish count bias associated with sampling range is reduced from 7.1 to 0.1.

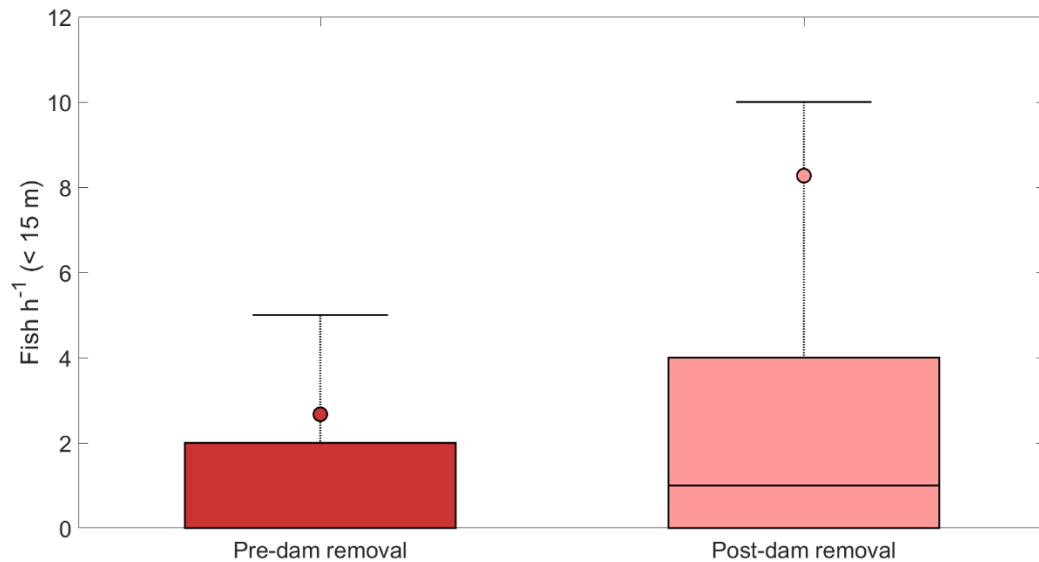
Figure 2.5. Fish h^{-1} metric (A) and fish $\text{h}^{-1} \text{m}^{-1}$ (B) metric compared by range sampled. Blue and red lines indicate the best fit line for each plot, respectively.



Fish abundance pre- and post-dam removal

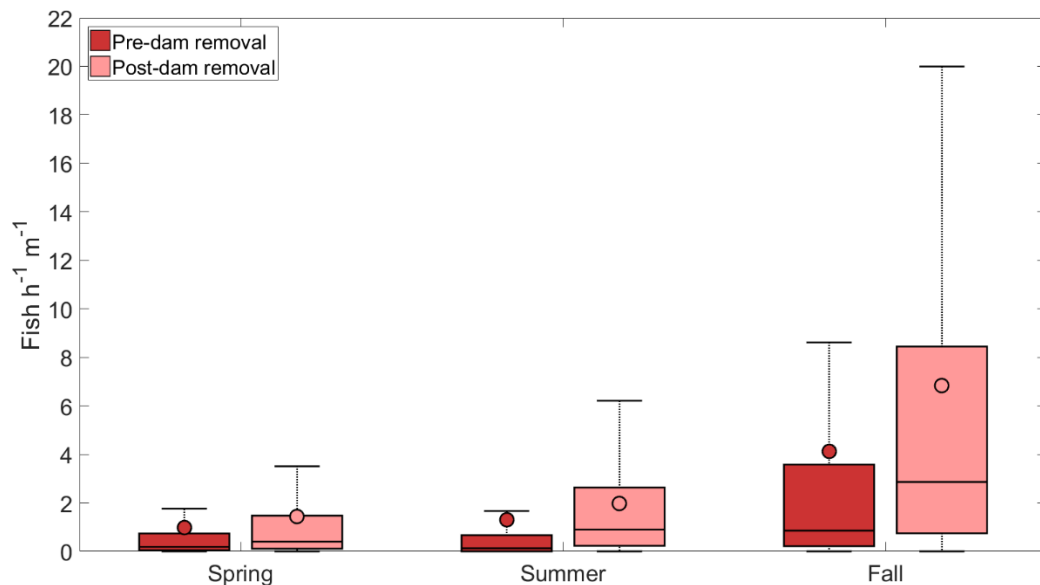
Fish counts (fish h^{-1}) within 15 m of the transducer increased during post-dam removal years relative to pre-dam removal years (Kruskal-Wallis $p < 0.001$; Figure 2.6). The mean of post-dam removal counts was 310% higher than pre-dam removal counts, while the 75th and 95th percentiles were 100% higher.

Figure 2.6. Fish tracks sampled within the first 15 meters of the transducer beam for all years pre- and post-dam removal. Box plots represent all fish counts detected within the first 15 m of the transducer for all years pre- and post-dam removal, respectively. $N_{\text{Pre-dam removal}} = 15,984$, $N_{\text{Post-dam removal}} = 18,888$. For each box plot, the black central line indicates the median, the bottom and top edges the 25th and 75th percentiles, respectively, and the top and bottom whiskers the 95th and 5th percentiles. The circles indicate means.



Range-corrected fish abundance changed seasonally with the highest being observed in the fall of all years sampled (Figure 2.7; Kruskal-Wallis, $p < 0.001$). Fish abundance in the spring and summer were significantly lower and less variable compared to the fall (Dunn-Sidak non-parametric post-hoc test, $p < 0.01$). Fish abundance by season was also significantly higher in post-dam removal years (Kruskal-Wallis, $p < 0.001$).

Figure 2.7. Fish abundance pre-and post-dam removal grouped by season. Box plot definitions are described in Figure 2.6. $N_{\text{Pre-dam removal}} (\text{Spring}; \text{Summer}; \text{Fall}) = 3,624; 5,616; 5,184$. $N_{\text{Post-dam removal}} (\text{Spring}; \text{Summer}; \text{Fall}) = 4,272; 6,480; 5,784$.



Continuous data revealed high variability in fish abundance for all years and river sides sampled (Figure 2.8). Fish abundances were higher in the fall for all years on both

river sides sampled. Lowest fish abundances were observed in the summer months (post summer solstice, June 21st, and before the autumn equinox, September 21st).

Figure 2.8. Recorded fish abundances (fish $h^{-1} m^{-1}$) in the Penobscot River for each year and river side sampled from 2010-2016. Blue areas indicate data gaps. Fish abundance and sampling range distributions for each collection year and river side are given in Table 2.4. Note that the limits on the y-axis are 0-100 fish $h^{-1} m^{-1}$ for Pen A and 0-40 fish $h^{-1} m^{-1}$ for Pen B.

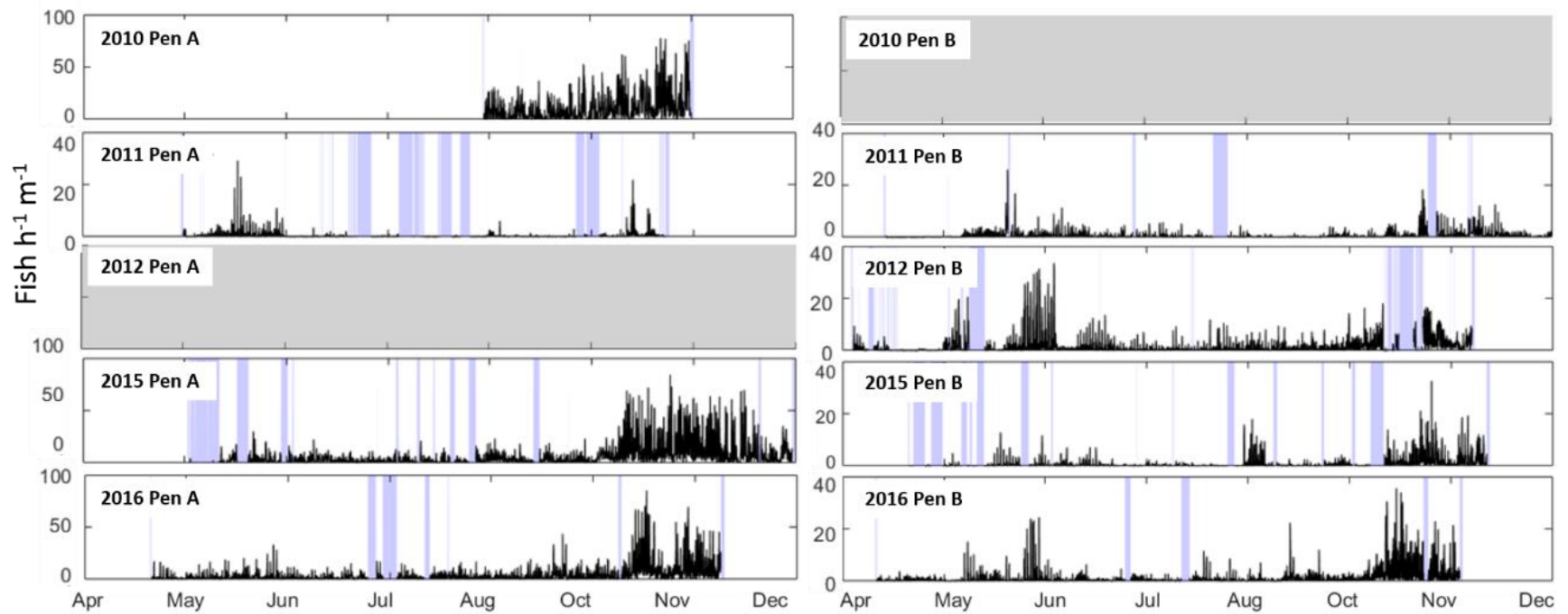


Table 2.4. Median fish abundance (fish h⁻¹ m⁻¹) and sampling range (m) broken down by year and river side.

		2010		2011		2012		2015		2016	
River side		A	B	A	B	A	B	A	B	A	B
<i>Fish h⁻¹ m⁻¹</i>	Median	6.18		0.06	0.18		0.56	2.89	0.14	2.08	0.38
	25 th %tile	1.98		0	0.05		0.21	0.98	0.04	0.78	0.13
	75 th %tile	15.08		0.28	0.58		1.68	7.47	0.53	4.93	1.05
<i>Range (m)</i>	Median	42.5		18.0	30.5		46.3	38.6	21.3	35.5	25.3
	25 th %tile	34.6		18.0	26.6		35.2	28.7	18.9	27.4	23.8
	75 th %tile	52.4		20.4	36.0		50.3	48.5	23.3	45.7	26.9

Pen A 2010 was only deployed in the fall months, when the highest relative fish abundances for each the year occurred, and displayed the greatest median sampling range among all years and river side sampled (Table 2.4).

Fish abundance and the environment

The most accurate, unpruned CART model resulted in a tree with 248 nodes with a relative predictive error of 0.55 ($R^2 = 0.484$). Briefly, the 3.4 times more targets were observed when day length was below 0.47, which roughly corroborates with the increased abundance observed in the Fall. Regardless of season, more fish were observed on river side Pen A than Pen B. Within the Fall season, roughly twice the number of targets were observed on an outgoing tide than an incoming tide. Of those targets leaving during the Fall on an outgoing tide, almost three times more targets were observed when

the temperature was below 11.6° C and those fish were more likely to migrate at night. Interestingly, dam removal was particularly useful in splitting relatively high temperature/low day length events, with roughly 8.7 times more targets after dam removal under these conditions. However, these conditions only account for 302 hours of the record. Finally, during high migration periods/high abundance events, higher discharge (>153 m³) was associated with the greatest number of observed fish abundance. Summer/spring abundance was generally lower and therefore more difficult to parse than Fall abundance with the CART approach.

The highest mean fish abundance (28.17 fish h⁻¹ m⁻¹) for a terminal node occurred during a time of year when daylength was less than 0.47 (~11.3 h), on the Pen A river side during an outgoing tide when water temperature was between 4.56 °C and 9.25 °C. The fish were moving at night (including dusk or dawn), water discharge was greater than 153 m³s⁻¹, and the moon phase was new, first quarter, or last quarter. A total of 110 sampling hours (of the total 31,642, 0.34% of the data) met these specific river conditions among all sampling years. The lowest mean fish abundance (0.014 fish h⁻¹ m⁻¹) occurred when daylength was greater than 0.56 (~13.4 h) and less than 0.64 (~15.4 h), located on the Pen A river side before dam removal, when water temperatures were greater than 21.8 °C, and fish were moving during the day during an outgoing tide. A total of 143 sampling hours met these specific river conditions.

Relative predictability scores for each environmental predictor were generated based on the unpruned decision tree (Table 2.5). Variables were scored based on the relative importance of each variable to the first splitter identified, which assumes a score of 100 (Table 2.5). The relative score of each variable is reflected in its usage as a splitter

node in the unpruned decision tree. Variables with higher scores produced greater differences in mean fish abundance detected. Daylength was the variable of highest importance with side of the river and temperature having similar scores. Water discharge and dam presence had approximately one quarter the predictive power of daylength. Tide phase and diel cycle, and moon phase had the lowest predictive power.

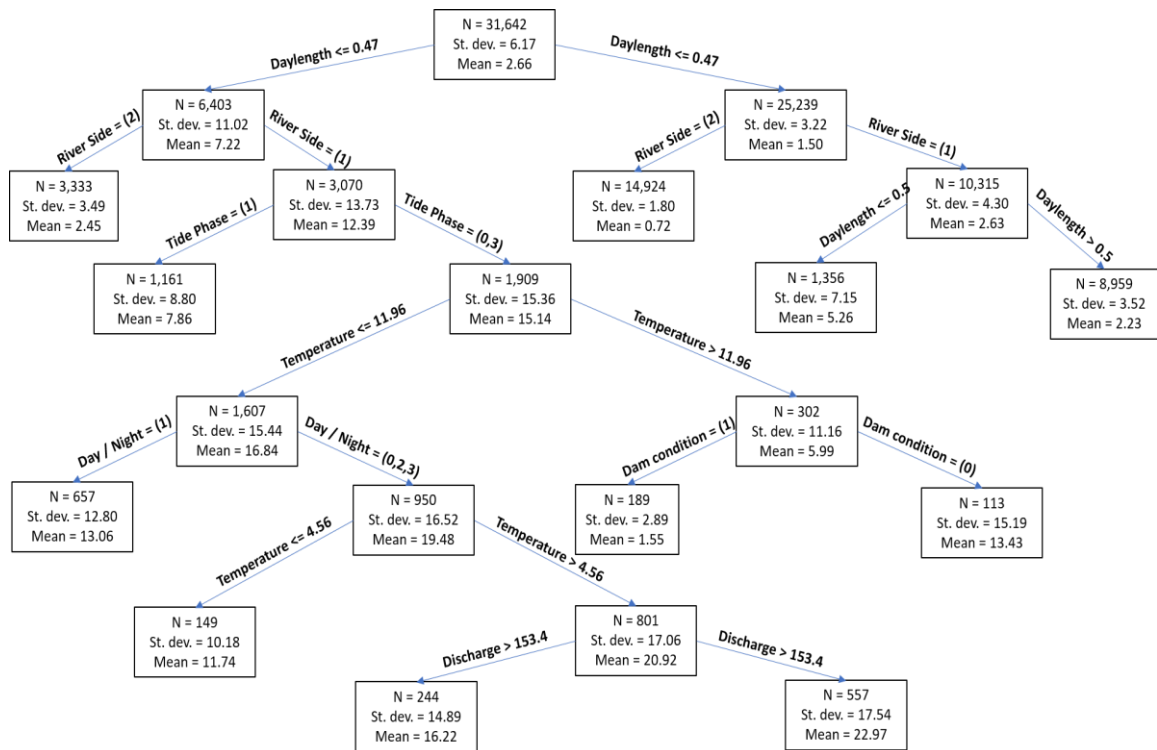
Table 2.5. Relative variable importance identified by the CART model with the highest relative predictability.

River Variable	Score
Daylength	100
River Side	76.17
Temperature	73.34
Discharge	24.83
Dam Condition	23.02
Tide Phase	18.78
Day/ Night	14.08
Moon Phase	7.50

The simplified decision tree was pruned to 21 nodes to visualize the exact conditions of the environmental variables that elicited the greatest response in fish abundances in the Penobscot River. It revealed that a daylength value of 0.47 produced the largest difference in mean fish abundance (Figure 2.9). The mean fish abundance detected during a daylength period over 0.47 of the day was 1.5 while the mean fish abundance with a daylength below 0.47 was 7.2 fish h⁻¹ m⁻¹. The next splitter identified

was river side, referring to the transducer systems on either side of the river (Pen A and B). The mean fish abundance on the Pen A river side was 12.4, while Pen B only averaged 2.5 fish h⁻¹ m⁻¹. Fish abundance detected on the Pen A river side was higher during outgoing tide and slack tide (15.12 fish h⁻¹ m⁻¹) than during incoming tide (7.88 fish h⁻¹ m⁻¹). Dam condition was found to produce a large difference in fish abundance for a subsample of 302 hours, where mean fish abundance was observed as 1.55 fish h⁻¹ m⁻¹ pre-dam removal and 13.43 fish h⁻¹ m⁻¹ post-dam removal.

Figure 2.9. Pruned decision tree created by CART analysis with a total of 21 nodes. The top node contains all data sampling hours (N = 31,642). N signifies the number of sampling hours contained within each node. The standard deviation of data contained in each node is also given. Specific river conditions applied to each node are indicated by the arrow pointing to the respective node.



DISCUSSION

This study addressed three distinct questions about fish presence and abundance in the Penobscot River: 1) did fish abundance increase in post-dam removal years relative to pre-dam removal years, 2) did fish abundances differ seasonally pre- and post-dam removal, and 3) how was fish abundances variability related to different environmental

conditions in the Penobscot River? The answers are yes, yes, and daylength, river side, temperature, discharge, and dam presence were most explanatory.

Fish abundances did increase post-dam removal and were clearly linked to specific seasons. Dam presence was an important indicator for fish abundance in the Penobscot River as total fish track counts within 15 m of the transducers increased in post-dam removal years (Figure 2.6), and post-dam removal years also had greater seasonal fish abundance (Figure 2.7). We hypothesized that fish abundance would increase post-dam removal based on other river restoration projects. For example, following a small dam removal in the Eightmile River system in Connecticut, enhanced river connectivity positively benefited fish assemblages and caused significant shifts in relative fish abundance over time (Poulos et al. 2014).

Increased fish abundance post-dam removal has also been found in parallel studies exploring species assemblage changes in the Penobscot River post-restoration, and by visual fish counts conducted at the respective lowermost dams in the Penobscot River. Kiraly et al. (2015) and Watson (2017) conducted electrofishing surveys from 2010 to 2012 (pre-dam removal) and 2014 to 2015 (post-dam removal) to study fish assemblages in the main stream and tributaries of the Penobscot River. River reaches that underwent habitat and connectivity changes post-dam removal displayed a 31% average increase in Morisita-Horn's species similarity index and was attributed to increased habitat access for anadromous fish (Watson 2017). An increase in total abundance for alewife, American shad, American eel, sea lamprey, and striped bass was revealed post-dam removal from visual fish counts conducted at the respective lowermost dam in the Penobscot River both pre- and post-dam removal (Veazie dam 2010 – 2013, Milford dam

2015-2016; Simpson, Mitchell, Maine Department of Marine Resources, unpublished data).

Increases in fish abundance for this and parallel studies cannot be disentangled from concurrent stocking efforts intended to “jump start” the increases in native fish populations anticipated after dam removal. As part of the overall objective of the Penobscot River Restoration Project to increase native fish abundances, adult alewife stocking efforts to lakes connected to the Penobscot River were recorded as: 12,378 in 2010; 3,734 in 2011; 48,648 in 2012; 32,775 in 2013; 43,204 in 2014; 56,506 in 2015, and 18,151 in 2016 (Cox et al. 2014). As such, production of juvenile alewife from these lakes has resulted in high fall emigration out of the Penobscot River. The high fish abundance we recorded in the fall cannot be separated into natural increases in fish numbers related to the dam removal and increases related to stocked adult production. This nuance must be considered when assessing the natural recovery of fish populations in the Penobscot River.

Many diadromous fish species with different migratory behaviors are present in the Penobscot River. The fish count metric applied in this study provided total fish abundance numbers over time, which was highly reflective of the most abundant species of fish present in the river, alewife. Biomass data, which in hydroacoustics translates to target strength (TS), is not included in the abundance metric used. While sporadic fish abundance peaks that occurred in June (Figure 2.8) are lower and span a shorter time period than fall abundance peaks, total biomass moving through the river at both of these times may be closer than the abundance metric indicates. June fish abundance peaks are likely to include adult anadromous fish migrating upriver to spawn (e.g., alewife, blue

back herring, shad, and Atlantic salmon), while fall peaks represent the spawned river herring juveniles for that year that are emigrating from the river and moving downstream in the fall. This scenario would certainly be plausible for alewife, as adult alewife migrate upriver to spawn in the late spring to early summer, and the young of the year begin their emigration to the sea in the fall of that same year (Mullen 1986).

Highest fish abundances were observed when daylength was less than 0.47 (11.3 hours), water temperature was between 4.56 °C and 9.25 °C, and discharge above 153 m³s⁻¹. These conditions indicate that the timing of these high fish abundance periods occurred during the fall i.e. from October 8th until the transducers were taken out. Fish species migrating in the fall are known to be influenced by seasonal river conditions (Tommasi et al. 2015). Discharge, water temperature, and daylight have previously been described to have a significant impact on migratory behavior and timing of various diadromous fishes (Jonsson 1991). Discharge influences the timing of Atlantic salmon smolt to initiate downstream migrations in the spring (Hesthagen and Garnås 1986), for example, as high discharge periods allow for reduced energy expenditure by increased flow velocity (Hanson and Jonnson 1985), and provides shelter from predators in form of decreased visibility caused by turbidity (Hvidsten and Hansen 1989). Smolt migrations of Atlantic salmon in the Ørkla River, Norway, have been found to be initiated by the first spring peak in water discharge (> 100 m³ s⁻¹) and continued to increase with increasing discharge (Hesthaven and Garnås 1986). The large increase in fish abundance detected during the fall months in the Penobscot River is likely a function of the migratory behavior of juvenile alewife. In addition to seasonal river conditions accentuating fall conditions for high fish abundance, periods with the greatest fish abundance were

specific to an outgoing tide, at night (including dusk or dawn), with a new, first quarter, or last quarter moon phase. This aligns with results from previous studies, which found that the onset of downstream migrating juvenile river herring (including alewife and blueback herring) occur mainly at night (Johnston and Cheverie 1988) with a new moon phase (Iafrate and Oliveira 2008).

No environmental variable can be described as a single migration trigger for an assemblage of diadromous species, or even a particular species. The smolt migrations in the Ørklå River, Norway are highly correlated with discharge (Garnås 1986). However, migrations of the same species were correlated with water temperature in the Imsa River, Norway (Jonsson and Ruud-Hansen 1985). The results from our CART analysis suggest that fish abundance in the Penobscot River is also influenced by a combination of environmental parameters, with daylength, temperature, tide phase, dam conditions, diel cycle, discharge, and moon phase all playing a role, but with different levels of significance (Table 2.5). Thereby, the categorical predictors of tide phase, diel cycle, moon phase, and dam condition have lower predictability scores than the continuous predictors of daylength, temperature, and discharge, partially because these variables do not undergo any seasonal variability. The categorical predictors used occur in the same form during both low and high fish abundance periods, thus lowering the predictability compared to variables that undergo seasonal changes.

River side is an artificial variable produced by our sampling procedure. CART identified river side as the second splitter, and second most important predictor of fish abundance. This indicates fish abundance on each river side differed significantly and could be due to any combination of 1) varying fish detection capabilities for each river-

side system to 2) differences in behavioral patterns of species preferring one river side over the other for their movement through this part of the river. Though it is evident that fish numbers detected by each river side are different, this study's focus was to develop a relative abundance index to assess changes in the Penobscot River from a pre- to a post-dam removal condition, and how the yearly variability in fish abundance observed might be linked to environmental conditions known to trigger fish migration behavior. CART analysis splitting fish abundance into two mutually exclusive groups by river side (Figure 2.9) assures us that relative fish abundance for each river condition (river side) is only being compared to the relative fish abundance collected on the same river side. Future studies involving river side counts could explore location preferences for fish, which may then be linked to the flow profile of the river, and a cross-sectional sampled species assemblage (as in Mitchell, 2006).

Standardizing fish abundance by range sampled does not completely remove the range bias associated with the fish detection probability at greater ranges (Figure 2.5B). While we are unable to correct for fish behavior, one possible solution to correct for the additional volume sampled at increasing range would be to calculate the volume sampled at each range and produce a metric of fish $\text{h}^{-1} \text{m}^{-3}$. The theoretical volume sampled by the acoustic beam for each hour would be estimated by calculating the volume of the acoustic cone given height and beam angle. The calculated volume would represent the volume sampled under optimal conditions. Given the dynamic nature of the river, and limitations of the acoustic sampling technique, it was determined that the optimal sampling volume was not reflective of the actual volume sampled at any time. As described in (Scherelis 2017), factors that influenced the volume sampled included the changing discharge of the

river, reflections from the river surface causing the geometric shape of the acoustic beam to change over time, and limited detection possibilities in the far-field of the beam due to “shadows” being produced by objects in the near-field beam. As many of these beam limitations were difficult to account for, especially over the entire sampling period, it was decided that we would accept the small error of standardizing fish counts by the range sampled (Figure 2.5B) to create a fish abundance metric, rather than attempting to standardize by volume, which would potentially produce a larger error by overcompensating for the volume gained. In other words, we decided to accept the inaccuracies of a known error, rather than risk incurring an unknown, potentially larger error.

Side-looking hydroacoustics are amenable to providing a hands-off indicator of a fish assemblage response to river restoration practices. The approach enabled an indicator of fish responses to a suite of river conditions over multiple years. Temporal patterns of fish abundance were deciphered and provided evidence of a trend that indicates an increase in fish abundances in post-dam removal years. Methods used to process these data (Chapter 1) allowed information for each fish track to be exported in an easily accessible format. Additional data collected available include detailed information about each fish track detected, including target strength, directionality, velocity, and depth. These data can be used in the future to study, for example, spatial usage of the river channel by fish, and more specific behavioral patterns of fish in relation to environmental conditions, such as directionality as a function of the diurnal cycle, tidal stage, or moon phase. Target strength can also be used to focus on a specific size class of fish (Boswell et al. 2008). The possibility for future studies focused on behavioral responses of fish at

the individual level using this dataset does exist, but would also require parallel methods to confirm the patterns observed. The tools presented here allowed continuous tracking of the progress of large restoration efforts that would allow researchers and managers to maximize limited investments on specific restoration objectives, e.g., dam removal in conjunction with stocking practices.

REFERENCES, CHAPTER 2

- Axenrot, T., Didrikas, T., Danielsson, C., Hansson, S. 2004. Diel patterns in pelagic fish behaviour and distribution observed from a stationary, bottom-mounted, and upward-facing transducer. *ICES Journal of Marine Science*. 61(7), 1100-1104.
- Boswell, K.M., Kaller, M.D., Cowan, J.H., Wilson, C.A. 2008. Evaluation of target strength-fish length equation choices for estimating estuarine fish biomass. *Hydrobiologia*, 610: 113-123.
- Breiman, L., Friedman, J.H., Olshen, R.A., Stone, C.J., 1984. *Classification and Regression Trees*. Chapman and Hall/CRC, New York.
- Burwen, D.L., Fleischman, S.J., Miller, J.D., Jensen, M.E. 2003. Time-based signal characteristics as predictors of fish size and species for a side-looking hydroacoustic application in a river. *ICES Journal of Marine Science*, 60(3), 662-668.
- Cairns, D. K., and D. G. Reddin. 2000. The potential impact of seal and seabird predation on North American Atlantic salmon. Department of Fisheries and Oceans, Canadian Stock Assessment Secretariat Research Document 2000/12, Ottawa.

- Cederholm, C. J., D. B. Houston, D. L. Cole, and W. J. Scarlett. 1989. Fate of coho salmon (*Oncorhynchus kisutch*) carcasses in spawning streams. *Canadian Journal of Fisheries and Aquatic Sciences* 46:1347–1355.
- Davies, P. E. and R. D. Sloane. 1987. Characteristics of the spawning migrations of brown trout, *Salmo trutta* L., and rainbow trout, *S. gairdneri* Richardson, in Great Lake, Tasmania. *Journal of Fish Biology*, 31: 353-373.
- Durbin, A. G., S. W. Nixon, and C. A. Oviatt. 1979. Effects of the spawning migration of the alewife, *Alosa pseudoharengus*, on freshwater ecosystems. *Ecology* 60:8–17.
- Gephard, S. 2008. Restoring Atlantic salmon (*Salmo salar*) to New England. Pages 75–84 in R. A. Askins, G. D. Dreyer, G. R. Visgilio, and D. M. Whitelaw, editors. *Saving biological diversity: balancing protection of the endangered species and ecosystems*. Springer Science, New York.
- Gewant, D., Bollens, S.M. 2012. Fish assemblages of interior tidal marsh channels in relation to environmental variables in the upper San Francisco Estuary. *Environmental Biology of Fishes*, 94:483-499.
- Hansen, L. P. and B. Jonsson. 1985. Downstream migration of hatchery-reared smolts of Atlantic salmon (*Salmo salar*) in the River Imsa, Norway. *Aquaculture*, 45: 237-248.
- Hesthagen, T. and E. Garnås. 1986. Migration of Atlantic salmon in River Ørkla of central Norway in relation to management of a hydroelectric station. *North American Journal of Fisheries Management*, 6: 376-382.

- Hvidsten, N. A. and L. P. Hansen. 1989. Increased recapture rate of adult Atlantic salmon, *Salmo salar* L., stocked as smolts at high water discharge. *Journal of Fish Biology*, 32: 153-154.
- Iafate, Joseph, and Kenneth Oliveira. 2008. Factors affecting migration patterns of juvenile river herring in a coastal Massachusetts stream. *Environmental Biology of Fishes*, 81.1: 101-110.
- Johnston, C. E. and J. C. Cheverie. 1988. Observations on the diel and seasonal drift of eggs and larvae of anadromous Rainbow smelt, *Osmerus mordax*, and Blueback Herring, *Alosa aestivalis*, in a coastal stream on Prince Edward Island. *Canadian Field Naturalist*, 102: 508-514.
- Jonsson, N. 1991. Influence of Water Flow, Water Temperature, and Light on Fish Migration in Rivers. *Nordic Journal of Freshwater Research*, 66: 20-35.
- Jonsson, B. and J. Ruud-Hansen. 1985. Water temperature as the primary influence on timing of seaward migrations of Atlantic salmon (*Salmo salar*) smolts. *Canadian Journal of Fisheries and Aquatic Sciences*, 42:593-595.
- Kiraly, I.A., Coghlan Jr., S.M., Zydlewski, J., Hayes, D. 2015. An assessment of fish assemblage structure in a large river. *River Research and Applications*, 31: 301-312.
- Kline, T. C. Jr., J. J. Goering, O. A. Mathisen, P. H. Poe, and P. L. Parker. 1990. Recycling of elements transported upstream by runs of Pacific salmon: I. $\delta^{15}\text{N}$ and $\delta^{13}\text{C}$ evidence in Sashin Creek, southeastern Alaska. *Canadian Journal of Fisheries and Aquatic Sciences*, 47:136-144.

- Martin, P. Rancon, J., Segure, G., Laffont, J., Boeuf, G., Dufour, S. 2012. Experimental study of the influence of photoperiod and temperature on the swimming behaviour of hatchery-reared Atlantic salmon (*Salmo salar* L.) smolts. *Aquaculture*, 362-363: 200-208.
- Mitchell, W.A. 2006. Estimating run size of anadromous fishes in the Roanoke River, North Carolina, using hydroacoustics. M.S. Thesis. North Carolina State University.
- Moring, J. R. 2005. Recent trends in anadromous fishes. Pages 25–42 in R. Buchsbaum, J. Pederson, and W. E. Robinson, editors. The decline of fisheries resources in New England: evaluating the impact of overfishing, contamination, and habitat degradation. Massachusetts Institute of Technology Sea Grant College Program, Publication 05-5, Cambridge.
- Mullen, D. M., C. W. Fay, and J. R. Moring. 1986. Species profiles: life histories and environmental requirements of coastal fishes and invertebrates (North Atlantic) alewife/blueback herring. U.S. Fish and Wildlife Service Biological Report 82(11.56). U.S. Army Corps of Engineers, TR EL-82-4.
- Opperman, J. J., Royte, J., Banks, J., Day, L. R., & Apse, C. 2011. The Penobscot River, Maine, USA: a basin-scale approach to balancing power generation and ecosystem restoration. *Ecology and Society*, 16(3): 7.
- Poulos, H.M., Miller, K.E., Kraczkowski, M.L. et al. 2014. Fish Assemblage Response to a Small Dam Removal in the Eightmile River System, Connecticut, USA. *Environmental Management* 54: 1090.

Rudstam, L.G., Jech, J.M., Parker-Stetter, S.L., Horne, J.K., Sullivan, P.J., Mason, D.M.

Pages 597 – 636 in A.V. Zale, D.L. Parrish, and T.M. Sutton, editors.2012.

Fisheries techniques, 3rd edition. American Fisheries Society, Bethesda,

Maryland.

Saunders, R. 2008. Penobscot River Long-term Ecological Monitoring: DRAFT NOAA

Priorities. February 20.

Saunders, R., Hachey, M.A., Fay, C.W. 2006. Maine's Diadromous Fish Community:

Past, Present, and Implications for Atlantic Salmon Recovery. Fisheries 31, 11:

537-547.

Schulze, M. B. 1996. Using a field survey to assess potential temporal and spatial overlap

between piscivores and their prey and a bioenergetics model to examine potential

consumption of prey, especially juvenile anadromous fish, in the Connecticut

River estuary. Master's thesis. University of Massachusetts, Amherst.

Sukhodolov, A. N. 2012. Structure of turbulent flow in a meander bend of a lowland

river, Water Resources Research, 48: 1-21.

Sumaila, U.R., Pitcher, T.J., Haggan, N., Jones, R. 2000. Evaluating the Benefits from

Restored Ecosystems: A Back to the Future Approach. IIFET Proceedings 1-7.

Thorpe, J. E., R. I. G. Morgan, D. Pretswell and P. J. Higgins. 1988. Movement rhythms

in juvenile Atlantic salmon (*Salmo salar*). Journal of Fish Biology, 33: 931-940.

Tommasi, D., Nye, J., Stock, C., Hare, J.A., Alexander, M., Drew, K. 2015. Effect of

environmental conditions on juvenile recruitment of alewife (*Alosa*

pseudoharengus) and blueback herring (*Alosa aestivalis*) in fresh water: a

- coastwide perspective. *Canadian Journal of Fisheries and Aquatic Sciences*, 72: 1037–1047.
- Trenkel V.M., Ressler, R.H., Jech, M., Giannoulaki, M., Tayler, C. 2001. Underwater acoustics for ecosystem-based management: state of the science and proposals for ecosystem indicators. *Marine Ecology Progress Series*, 442: 285-301.
- Trinko-Lake, T. R., Ravana, K. R., & Saunders, R. 2012. Evaluating changes in diadromous species distributions and habitat accessibility following the Penobscot River Restoration Project. *Marine and Coastal Fisheries*, 4(1), 284-293.
- Vollestad, L. A., B. Jonsson, N. A. Hvidsten, T. F. Næsje, O. Haraldstad and J. Ruud-Hansen. 1986. Environmental factors regulating the seaward migration of European silver eels (*Anguilla anguilla*). *Canadian Journal of Fisheries and Aquatic Sciences*, 43: 1909-1916.
- Watson, J. 2017. Dam removal and fish passage improvement influence fish assemblages in the Penobscot River, Maine. Master's thesis. University of Maine, Orono.
- Cox, O. Wipfelhauser, G., Dill, R., Bartlett, J., Lazzari, M. 2015. Restoration and monitoring of diadromous fish in Maine Annual Progress Report. FBMS#F14AF00183.
- Wood, C. C. 1986. Dispersion of common merganser (*Mergus merganser*) breeding pairs in relation to the availability of juvenile Pacific salmon in Vancouver Island streams. *Canadian Journal of Zoology*, 64: 756–765.

Zydlewski, G. B., Staines, G. In preparation. A biological indicator for large river restoration: Overcoming the challenges of applying fisheries acoustics in a tidal river. for: Ecological Applications.

Zydlewski, G.B., Zydlewski, J. 2012. Gill Na⁺,K⁺-ATPase of Atlantic salmon smolts in freshwater is not a predictor of long-term growth in seawater. *Aquaculture*, 362-363: 121-126.

BIBLIOGRAPHY

- Axenrot, T., Didrikas, T., Danielsson, C., Hansson, S. 2004. Diel patterns in pelagic fish behaviour and distribution observed from a stationary, bottom-mounted, and upward-facing transducer. *ICES Journal of Marine Science*. 61(7), 1100-1104.
- Baldwin, C. M., and J. G. McLellan. 2008. Use of gill nets for target verification of a hydroacoustic fisheries survey and comparison with kokanee spawner escapement estimates from a tributary trap. *North American Journal of Fisheries Management*, 28: 1744-1757.
- Ballón, M., Bertranda, A., Lebourges-Dhaussyc, A., Gutiérrezd, M., Ayóna, P., Gerlottob, D.G.F. 2011. *Progress in Oceanography*, 91: 360-381.
- Banneheka, S.G., Routledge, R.D., Guthrie, I.C., Woodey, J.C. 1995. Estimation of in-river fish passage using a combination of transect and stationary hydroacoustic sampling. *Canadian Journal of Fisheries and Aquatic Sciences*, 52: 335-343.
- Bentley, N., Kendrick, T.H., Starr, P.J., Breen, P.A. 2011 Influence plots and metrics: tools for better understanding fisheries catch-per-unit-effort standardizations. *ICES Journal of Marine Science*, 69: 84-88.
- Boswell, K.M., Kaller, M.D., Cowan, J.H., Wilson, C.A. 2008. Evaluation of target strength-fish length equation choices for estimating estuarine fish biomass. *Hydrobiologia*, 610: 113-123.
- Breiman, L., Friedman, J.H., Olshen, R.A., Stone, C.J., 1984. *Classification and Regression Trees*. Chapman and Hall/CRC, New York.
- Burwen, D.L., Fleischman, S.J., Miller, J.D., Jensen, M.E. 2003. Time-based signal characteristics as predictors of fish size and species for a side-looking hydroacoustic application in a river. *ICES Journal of Marine Science*, 60(3), 662-668.
- Cairns, D. K., and D. G. Reddin. 2000. The potential impact of seal and seabird predation on North American Atlantic salmon. Department of Fisheries and Oceans, Canadian Stock Assessment Secretariat Research Document 2000/12, Ottawa.
- Cederholm, C. J., D. B. Houston, D. L. Cole, and W. J. Scarlett. 1989. Fate of coho salmon (*Oncorhynchus kisutch*) carcasses in spawning streams. *Canadian Journal of Fisheries and Aquatic Sciences* 46:1347–1355.
- Cox, O. Wipfelhauser, G., Dill, R., Bartlett, J., Lazzari, M. 2015. Restoration and monitoring of diadromous fish in Maine Annual Progress Report. FBMS#F14AF00183.

- Daum, D.W., Osborne, B.M. 1998. Use of fixed-location, split-beam sonar to describe temporal and spatial patterns of adult fall chum salmon migration in the Chandalar River, Alaska. *North American Journal of Fisheries Management*, 18: 477-486.
- Davies, P. E. and R. D. Sloane. 1987. Characteristics of the spawning migrations of brown trout, *Salmo trutta* L., and rainbow trout, *S. gairdneri* Richardson, in Great Lake, Tasmania. *Journal of Fish Biology*, 31: 353-373.
- De Robertis, A.D., Higginbottom, I. 2007. A post-processing technique to estimate the signal- to-noise ratio and remove echosounder background noise. *ICES Journal of Marine Science*, 64: 1282- 1291.
- Durbin, A. G., S. W. Nixon, and C. A. Oviatt. 1979. Effects of the spawning migration of the alewife, *Alosa pseudoharengus*, on freshwater ecosystems. *Ecology* 60:8–17.
- Echoview Manual Pty Ltd (2015). Echoview software, version 6.1.44. Echoview Software Pty Ltd, Hobart, Australia.
- Fraser, S., Nikora, V., Williamson, B.J., Scott, B.E. 2017. Automatic active acoustic target detection in turbulent aquatic environments. *Limnology and Oceanography: Methods*, 00: 00-00.
- Frear, P.A. 2002. Hydroacoustic target strength validation using angling creel census data. *Fisheries Management and Ecology*, 9: 343-350.
- Gephard, S. 2008. Restoring Atlantic salmon (*Salmo salar*) to New England. Pages 75–84 in R. A. Askins, G. D. Dreyer, G. R. Visgilio, and D. M. Whitelaw, editors. *Saving biological diversity: balancing protection of the endangered species and ecosystems*. Springer Science, New York.
- Gewant, D., Bollens, S.M. 2012. Fish assemblages of interior tidal marsh channels in relation to environmental variables in the upper San Francisco Estuary. *Environmental Biology of Fishes*, 94:483-499.
- Hansen, L. P. and B. Jonsson. 1985. Downstream migration of hatchery-reared smolts of Atlantic salmon (*Salmo salar*) in the River Imsa, Norway. *Aquaculture*, 45: 237-248.
- Hartman, K.J., Nagy, B., Tipton, R.C., Morrison, S. 2000. Verification of hydroacoustic estimates of fish abundance in Ohio River lock chambers. *North American Journal of Fisheries Management*, 20: 1049-1056.
- Hesthagen, T. and E. Garnås. 1986. Migration of Atlantic salmon in River Ørkla of central Norway in relation to management of a hydroelectric station. *North American Journal of Fisheries Management*, 6: 376-382.

- Hughes, J.B., Hightower, J.E. Combining split- beam and dual- frequency identification sonars to estimate abundance of anadromous fish in the Roanoke River, North Carolina. *North American Journal of Fisheries Management*, 35: 229-240.
- Hvidsten, N. A. and L. P. Hansen. 1989. Increased recapture rate of adult Atlantic salmon, *Salmo salar* L., stocked as smolts at high water discharge. *Journal of Fish Biology*, 32: 153-154.
- Iafraite, Joseph, and Kenneth Oliveira. 2008. Factors affecting migration patterns of juvenile river herring in a coastal Massachusetts stream. *Environmental Biology of Fishes*, 81.1: 101-110.
- Johnston, C. E. and J. C. Cheverie. 1988. Observations on the diel and seasonal drift of eggs and larvae of anadromous Rainbow smelt, *Osmerus mordax*, and Blueback Herring, *Alosa aestivalis*, in a coastal stream on Prince Edward Island. *Canadian Field Naturalist*, 102: 508-514.
- Jonsson, B. and J. Ruud-Hansen. 1985. Water temperature as the primary influence on timing of seaward migrations of Atlantic salmon (*Salmo salar*) smolts. *Canadian Journal of Fisheries and Aquatic Sciences*, 42:593-595.
- Jonsson, N. 1991. Influence of Water Flow, Water Temperature, and Light on Fish Migration in Rivers. *Nordic Journal of Freshwater Research*, 66: 20-35.
- Kendrick T. H., Bentley N. 2010. Fishery characterization and catch-per-unit-effort indices for trevally in TRE 7, 1989-90 to 2007-08. *New Zealand Fisheries Assessment Report*, 2010/41pg. 58 pp.
- Kieser, R., Reynisson, P., and Mulligan, T. J. 2005. Definition of signal-to-noise ratio and its critical role in split-beam measurements. *ICES Journal of Marine Science*, 62: 123–130.
- Kiraly, I.A., Coghlan Jr., S.M., Zydlewski, J., Hayes, D. 2015. An assessment of fish assemblage structure in a large river. *River Research and Applications*, 31: 301-312.
- Klevjer, T.A., Kaartvedt, S. 2003. Split-beam target tracking can be used to study the swimming behavior of deep-living plankton in situ. *Aquatic Living Resources*, 16: 293 -298.
- Kline, T. C. Jr., J. J. Goering, O. A. Mathisen, P. H. Poe, and P. L. Parker. 1990. Recycling of elements transported upstream by runs of Pacific salmon: I. $\delta^{15}\text{N}$ and $\delta^{13}\text{C}$ evidence in Sashin Creek, southeastern Alaska. *Canadian Journal of Fisheries and Aquatic Sciences*, 47:136–144.
- Koslow, A.J. 2009. The role of acoustics in ecosystem- based fishery management. *ICES Journal of Marine Science*, 66: 966-973.

- Krumme, U. 2004. Patterns in tidal migration of fish in a Brazilian mangrove channel as revealed by a split-beam echosounder. *Fisheries Research*, 70: 1-15.
- Love, R.H. 1977. Target strength of an individual fish at any aspect. *Journal of the Acoustical Society of America*, 62: 1397-1403.
- Mann, D. A., Hawkins, A. D., & Jech, J. M. (2008). Active and passive acoustics to locate and study fish. In *Fish bioacoustics* (pp. 279-309). Springer New York.
- Martin, P. Rancon, J., Segure, G., Laffont, J., Boeuf, G., Dufour, S. 2012. Experimental study of the influence of photoperiod and temperature on the swimming behaviour of hatchery-reared Atlantic salmon (*Salmo salar* L.) smolts. *Aquaculture*, 362-363: 200-208.
- Maxwell, S.L., Gove, N.E. 2008. Assessing a dual-frequency identification sonar's fish-counting accuracy, precision, and turbid river range capability. *The Journal of the Acoustical Society of America*, 122: 3364-3377.
- Misund, O.A., Beltestad, A.K. 1996. Target-strength estimates of schooling herring and mackerel using the comparison method. *ICES Journal of Marine Science*, 53: 281-284.
- Mitchell, W.A. 2006. Estimating run size of anadromous fishes in the Roanoke River, North Carolina, using hydroacoustics. M.S. Thesis. North Carolina State University.
- Mitson, R. B., and Knudsen, H. P. 2003. Causes and effects of underwater noise on fish-abundance estimation. *Aquatic Living Resources*, 16: 255-263.
- Moring, J. R. 2005. Recent trends in anadromous fishes. Pages 25–42 in R. Buchsbaum, J. Pederson, and W. E. Robinson, editors. *The decline of fisheries resources in New England: evaluating the impact of overfishing, contamination, and habitat degradation*. Massachusetts Institute of Technology Sea Grant College Program, Publication 05-5, Cambridge.
- Mullen, D. M., C. W. Fay, and J. R. Moring. 1986. Species profiles: life histories and environmental requirements of coastal fishes and invertebrates (North Atlantic) alewife/blueback herring. U.S. Fish and Wildlife Service Biological Report 82(11.56). U.S. Army Corps of Engineers, TR EL-82-4.
- Opperman, J. J., Royte, J., Banks, J., Day, L. R., & Apse, C. 2011. The Penobscot River, Maine, USA: a basin-scale approach to balancing power generation and ecosystem restoration. *Ecology and Society*, 16(3): 7.
- Osborne, B.M., Melegari, J.L. 2002. Use of split-beam sonar to enumerate Chandalar River fall chum salmon, 2000. Alaska Fisheries Technical Report Number 61.

- Poulos, H.M., Miller, K.E., Kraczkowski, M.L. et al. 2014. Fish Assemblage Response to a Small Dam Removal in the Eightmile River System, Connecticut, USA. *Environmental Management* 54: 1090.
- Rudstam, L.G., Jech, J.M., Parker-Stetter, S.L., Horne, J.K., Sullivan, P.J., Mason, D.M. Pages 597 – 636 in A.V. Zale, D.L. Parrish, and T.M. Sutton, editors. 2012. *Fisheries techniques*, 3rd edition. American Fisheries Society, Bethesda, Maryland.
- Rudstam, L.G., Schaner, T., Gal, G. Boscarino, B.T., O’Gorman, R., Warner, D.M., Johannsson, O.E., Bowen, K.L. 2008. Hydroacoustic measures of *Mysis relicta* abundance and distribution in Lake Ontario. *Aquatic Ecosystem Health & Management*, 11: 355-367.
- Samedy, V., Wach, M., Lobry, J., Selleslagh, J., Pierre, M., Josse, E., Boët, P. 2015. Hydroacoustics as a relevant tool to monitor fish dynamics in large estuaries. *Fisheries Research*, 172: 225-233.
- Saunders, R. 2008. Penobscot River Long-term Ecological Monitoring: DRAFT NOAA Priorities. February 20.
- Saunders, R., Hachey, M.A., Fay, C.W. 2006. Maine’s Diadromous Fish Community: Past, Present, and Implications for Atlantic Salmon Recovery. *Fisheries* 31, 11: 537-547.
- Schulze, M. B. 1996. Using a field survey to assess potential temporal and spatial overlap between piscivores and their prey and a bioenergetics model to examine potential consumption of prey, especially juvenile anadromous fish, in the Connecticut River estuary. Master’s thesis. University of Massachusetts, Amherst.
- Scoulding, B., Chu, D., Ona, E., Fernandes, P.G. 2015. Target strengths of two abundant mesopelagic fish species. *Journal of the Acoustical Society of America*, 137: 989-1000.
- Similä, T. 1997. Sonar observations of killer whales (*Orcinus orca*) feeding on herring schools. *Aquatic Mammals*, 23: 119-126.
- Simmonds, J., MacLennan, D. 2005. Biological Acoustics. In *Fisheries Acoustics Theory and Practice*, 2nd edn, pp. 158-162. Blackwell Science, Oxford, UK.
- Steig, T.W., Nealson, P.A., Sullivan, C.M., Ehrenberg, J.E. 2010. Development of a method for estimating the probability of detecting fish through a hydroacoustic beam. *Oceans 2010 MTS/IEEE Seattle*, Seattle, WA: 1-13.
- Sukhodolov, A. N. 2012. Structure of turbulent flow in a meander bend of a lowland river, *Water Resources Research*, 48: 1-21.

- Sumaila, U.R., Pitcher, T.J., Haggan, N., Jones, R. 2000. Evaluating the Benefits from Restored Ecosystems: A Back to the Future Approach. IIFET Proceedings 1-7.
- Swartzman, G., Silverman, E., Williamson, N. 1995. Relating trends in walleye pollock (*Theragra chalcogramma*) abundance in the Bering Sea to environmental factors. Canadian Journal of Fisheries and Aquatic Sciences, 52: 369-380.
- Thorpe, J. E., R. I. G. Morgan, D. Pretswell and P. J. Higgins. 1988. Movement rhythms in juvenile Atlantic salmon (*Salmo salar*). Journal of Fish Biology, 33: 931-940.
- Tommasi, D., Nye, J., Stock, C., Hare, J.A., Alexander, M., Drew, K. 2015. Effect of environmental conditions on juvenile recruitment of alewife (*Alosa pseudoharengus*) and blueback herring (*Alosa aestivalis*) in fresh water: a coastwide perspective. Canadian Journal of Fisheries and Aquatic Sciences, 72: 1037–1047.
- Trenkel V.M., Ressler, R.H., Jech, M., Giannoulaki, M., Tayler, C. 2001. Underwater acoustics for ecosystem-based management: state of the science and proposals for ecosystem indicators. Marine Ecology Progress Series, 442: 285-301.
- Trinko-Lake, T. R., Ravana, K. R., & Saunders, R. 2012. Evaluating changes in diadromous species distributions and habitat accessibility following the Penobscot River Restoration Project. Marine and Coastal Fisheries, 4(1), 284-293.
- Viehman, H.A., Zydlewski, G.B., McCleave, J.D., Staines, G.J. 2015. Using hydroacoustics to understand fish presence and vertical distribution in a tidally dynamic region targeted for energy extraction. Estuaries and Coasts, 38: 215-226.
- Vollestad, L. A., B. Jonsson, N. A. Hvidsten, T. F. Næsje, O. Haraldstad and J. Ruud-Hansen. 1986. Environmental factors regulating the seaward migration of European silver eels (*Anguilla anguilla*). Canadian Journal of Fisheries and Aquatic Sciences, 43: 1909-1916.
- Watson, J. 2017. Dam removal and fish passage improvement influence fish assemblages in the Penobscot River, Maine. Master's thesis. University of Maine, Orono.
- Wood, C. C. 1986. Dispersion of common merganser (*Mergus merganser*) breeding pairs in relation to the availability of juvenile Pacific salmon in Vancouver Island streams. Canadian Journal of Zoology, 64: 756–765.
- Zhang, J., Zuo-zhi, C., Guo-bao, C., Peng, Z., Yong-song, Q., Zhuang, Y. 2015. Hydroacoustic studies on the commercially important squid *Sthenoteuthis oualaniensis* in the South China Sea. Fisheries Research, 169: 45-51.
- Zydlewski, G. B., Staines, G. In preparation. A biological indicator for large river restoration: Overcoming the challenges of applying fisheries acoustics in a tidal river. for: Ecological Applications.

Zydlewski, G.B., Zydlewski, J. 2012. Gill Na⁺,K⁺-ATPase of Atlantic salmon smolts in freshwater is not a predictor of long-term growth in seawater. *Aquaculture*, 362-363: 121-126.

BIOGRAPHY OF THE AUTHOR

Constantin Carl Scherelis was born on September 29, 1992 in Gifhorn, Germany. He grew up in Braunschweig, Germany, and attended a German high school (Gymnasium) up to his junior year. Constantin then moved to Portland, Oregon, USA as an exchange student to complete his junior year of high school. Family circumstances caused him to move to Chattanooga, Tennessee, USA for his senior year of high school instead of continuing his schooling in Germany, as originally planned. After graduating from Baylor School in 2010, he attended the University of Tennessee at Knoxville, where he graduated *cum laude* with a B.S. in Geology and Environmental Studies in the Honors track. During his time at the University of Tennessee, Constantin was also part of the Higher Education and Research Experience (HERE) program at Oak Ridge National Laboratory (ORNL) from 2011-2014. As part of the environmental sciences division at ORNL, he contributed to several research projects conducted on the effects of marine hydrokinetic turbines on fish behavior, and how fish respond in the proximity of these turbines. Constantin became proficient in the use of hydroacoustics as a fisheries research tool during his time at Oak Ridge National Laboratory, which made him a good candidate for a Master's project at the University of Maine. He is a candidate for the Master of Science degree in Oceanography from the University of Maine in August 2017.